Results in Physics 61 (2024) 107719

Contents lists available at ScienceDirect

Results in Physics

journal homepage: www.elsevier.com/locate/rinp

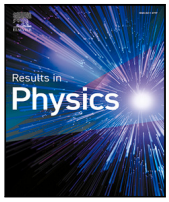

Status report on global pulsar-timing-array efforts to detect gravitational waves

Joris P.W. Verbiest [a,*], Sarah J. Vigeland [b], Nataliya K. Porayko [c,d], Siyuan Chen [e,f], Daniel J. Reardon [g,h]

[a] Florida Space Institute, University of Central Florida, 12354 Research Parkway, Orlando, 32826, FL, USA
[b] Center for Gravitation, Cosmology and Astrophysics, Department of Physics, University of Wisconsin-Milwaukee, P.O. Box 413, Milwaukee, 53201, WI, USA
[c] Dipartimento di Fisica "G. Occhialini", Universita degli Studi di Milano-Bicocca, Piazza della Scienza 3, Milano, 20126, Italy
[d] Max–Planck-Institut fuer Radioastronomie, Auf dem Huegel 69, Bonn, 53121, Germany
[e] Shanghai Astronomical Observatory, Chinese Academy of Sciences, 80 Nandan Road, Shanghai, 200030, PR China
[f] Kavli Institute for Astronomy and Astrophysics, Peking University, 5 Yiheyuan Road, Beijing, 100871, PR China
[g] Centre for Astrophysics and Supercomputing, Swinburne University of Technology, P.O. Box 218, Hawthorn, VIC 3122, Australia
[h] OzGrav: The Australian Research Council Centre of Excellence for Gravitational Wave Discovery, Hawthorn, VIC 3122, Australia

ARTICLE INFO

Keywords:
Pulsar timing array
Gravitational waves
IISM
Gravitational wave detection

ABSTRACT

The stability of the spin of pulsars and the precision with which these spins can be determined, allows many unique tests of interest to physics and astrophysics. Perhaps the most challenging and revolutionary of these, is the detection of nanohertz gravitational waves. An increasing number of efforts to detect and study long-period gravitational waves by timing an array of pulsars have been ongoing for several decades and the field is moving ever closer to actual gravitational-wave science. In this review article, we summarize the state of this field by presenting the current sensitivity to gravitational waves and by reviewing recent progress along the multiple lines of research that are part of the continuous push towards greater sensitivity. We also briefly review some of the most recent efforts at astrophysical interpretation of the most recent GW estimates derived from pulsar timing.

Introduction

When the cores of moderately massive stars collapse after nuclear fusion ceases, neutron stars can be formed. These objects conserve a lot of the original angular moment of the progenitor star, but are far more compact, leading to rapid spins on the order of fractions of a second. A significant number of these neutron stars furthermore preserve their binary companion stars and can gain further angular momentum when this companion star evolves into a red giant — this is the generally agreed way in which so-called millisecond pulsars (MSPs) are created [1].

Many neutron stars can be detected on Earth due to radiation that is emitted along their magnetic field lines. While the exact emission mechanism is not fully understood to date [2], the "lighthouse model" of pulsar emission is undisputed. It posits that the magnetic axis of the neutron star is misaligned with the rotation axis and that consequently the radiation that emanates from the magnetic pole is swept around in space like the beam from a lighthouse. If the Earth is fortunate to be positioned within that sweeping cone of emission, the neutron star can be observed as a series of radiation pulses, in which case the object is typically referred to as a pulsar [3].

Due to the extremely stable spin, the pulsar's sequence of pulses that can be observed on Earth is typically extremely predictable. While there are a variety of perturbing effects observable in "slow" pulsars [4], the MSPs tend to be highly predictable. Consequently, these pulses can be used to determine a so-called pulsar-timing model which mathematically describes all effects that impact the arrival time of a pulsar's pulses on Earth. Such effects include obviously the spin period and the period derivative (due to energy loss) of the pulsar, but also a description of the binary orbit the pulsar might inhabit (often including relativistic orbital effects), delays incurred during propagation through the ionized interstellar medium and astrometric properties like the position, proper motion and distance of the pulsar to Earth. Through fitting of the timing model to the arrival times of the pulses at the observatory, any and all of the aspects affecting the timing model can be studied in great detail, see Lorimer and Kramer [5] for a review.

Probably the most prized phenomenon that could affect the times-of-arrival (ToAs) of pulsar pulses, is the stretching and squeezing of

* Corresponding author.
E-mail address: Joris.Verbiest@ucf.edu (J.P.W. Verbiest).

https://doi.org/10.1016/j.rinp.2024.107719
Received 15 January 2024; Received in revised form 13 April 2024; Accepted 29 April 2024
Available online 4 May 2024

space–time by gravitational waves (GWs). The fact that these exotic predictions of general relativity would impact pulsar ToAs has been appreciated since the late 1970s [6,7], although in principle it would be hard to differentiate those signals from many other noise sources in the measurement data (see Section "Noise Analysis"). Hellings and Downs [8] provided the solution to this problem, by deriving the mathematical prediction of the *correlated* signal incurred by ToAs due to GWs. Specifically, Hellings and Downs [8] demonstrated that the GW impact would display a nearly quadrupolar correlation signature as a function of the angular separation between the pulsars whose data are being correlated. This idea of hunting for a signal that is not uniquely identifiable within the data set of a single pulsar, but that can only be detected through timing of multiple pulsars, gave rise to the idea of the *pulsar timing array (PTA)*, which was first proposed by Foster and Backer [9] and Romani [10]. Specifically, they proposed that three unique signals could be pulled from timing an array of pulsars: monopolar correlations would relate to imperfections in the clock standards used [11], dipolar correlations would relate to errors in the Solar-System ephemerides used [12–14] and finally, quadrupolar correlations would be caused by gravitational waves.

A number of reviews have been published related to the concept and workings of PTAs. Since the present article is mostly interested in providing an overview of recent results, we will refer the interested reader now to review articles that cover other aspects of PTA experiments. The most comprehensive and recent review is the book by Taylor [15], which covers particularly the theory and software used for GW detection with PTAs in great detail. A more introductory overview can be found in Verbiest et al. [16] and a somewhat shorter treatment that includes a review of the state of the art in PTA research nearly a decade ago, is given by Lommen [17]. A basic review article that includes an overview of the various software packages that were used in PTA research half a decade ago, can be found in Hobbs and Dai [18]. Tiburzi [19] presents an overview of the PTA concept, with particular focus on various aspects directly related to pulsar timing. A thorough review of the astrophysical sources of GWs that could be detectable by PTAs was recently published by Burke-Spolaor et al. [20], while the theoretical treatment of how the different types of sources impact the timing measurements can be found in Perrodin and Sesana [21]. Finally, a comprehensive description of the many factors that drive measurement uncertainty in PTA work was provided by Verbiest and Shaifullah [4].

In this paper, we will review the recent progress in PTA research. Specifically, in Section "The PTA Landscape", we will briefly summarize the various efforts that are being undertaken around the world to detect GWs in PTA data. Section "Steps in the PTA Process" will provide an overview of the aspects that compose the entirety of PTA science; and the state-of-the-art of each of these aspects will be further described in subsequent sections: existent data sets (Section "PTA Data Sets"), timing software (Section "Pulsar Timing Software"), noise modeling (Section "Noise Analysis") and current challenges including various propagation delays (Section "Current Challenges"). The current state of published GW results from PTAs is given in Section "Signals and Detections" and in Section "Astrophysical Interpretation", we will briefly summarize the astrophysical implications of those results. In Section "Anticipated Improvements" we will present a few of the most eagerly anticipated developments in PTA research and finally, in Section "Discussion and Conclusions" we sum up the most pertinent points of this review.

The PTA landscape

Even though the concept of PTAs has been around since the late 1980s, at that time the practical implementation was effectively impossible. By 1990, only eight MSPs were known. Four of those MSPs (PSRs B1821−24 A, B1620−26, B1516+02 A and B1516+02B) inhabited globular clusters — such pulsars are randomly accelerated in the highly dense gravitational environment and can therefore not be timed with high precision. Of the remaining four MSPs, one (PSR B1957+20) inhabited a so-called "black-widow" system in which the ultra-light companion star was believed to be stripped apart, causing the orbit (and hence the timing) to be highly unstable.[1] The original MSP, PSR B1937+21, also did not possess the high timing stability required for PTA experiments, even though on short time scales (weeks to months) its precision was phenomenal, due to its high brightness. This left only two MSPs that could realistically be used for PTA experiments, which was insufficient for allowing the detection of any correlated signal.

A number of highly successful pulsar surveys in the Southern hemisphere changed this situation from the mid-1990s onwards. The Parkes-70 cm survey [24] discovered 18 new MSPs in the Galactic disk, the Parkes Multibeam Pulsar Survey [25] discovered 30 new MSPs and simultaneously, the Parkes-Swinburne Multibeam Survey [26] found another 20 MSPs. In total, by the end of 2005, no less than 67 MSPs were known in the Milky Way and very soon the first monitoring results indicated that the timing precision and stability of many of these objects was sufficient to make PTA research a realistic endeavor [27].

The success of the Parkes telescope in these pulsar surveys was primarily due to its opportune position in the Southern hemisphere, from where the Galactic centre can be seen. Since most pulsars inhabit the Galactic disk [even if MSPs have a somewhat higher scale height than most heavy stars, see 28], this placed Parkes in a unique position and consequently they were the first to formally set up a pulsar timing array: the Parkes Pulsar Timing Array or PPTA [29], soon followed by the European Pulsar Timing Array or EPTA [23] and the North-American Nanohertz Observatory for Gravitational Waves or NANOGrav [30]. Even though all these PTAs were formally started in the first decade of the new millennium, many use data from pulsar-monitoring campaigns that predate the formal founding of the projects, which means that many of the PTA data sets date back to the mid-90s or even earlier. Soon after these three original PTAs commenced operations, the scientific benefit of international collaboration in this high-demands and high-stakes project was recognized, which led to the founding of the International Pulsar Timing Array or IPTA. A description of the organizational set-up of the IPTA, especially in those earlier days, can be found in Manchester [31], a more comprehensive description of their observing programs and sensitivity was given in Verbiest et al. [32] and updated in Perera et al. [33].

In more recent years, new and upgraded telescopes have joined the PTA endeavor. Specifically the upgraded Giant Metre-Wave Radio Telescope (uGMRT) in India forms the Indian Pulsar Timing Array or InPTA [34,35], which formally joined the IPTA in 2022. The Five-hundred metre Aperture Spherical Telescope (FAST) forms the backbone for the recently established Chinese Pulsar Timing Array [CPTA 36], which is planning to also incorporate the 110-m Qitai Radio Telescope (QTT). The relatively new MeerKAT telescope array in South Africa also recently commenced its own PTA program, the MeerKAT Pulsar Timing Array or MPTA [37]. The MPTA and CPTA have not formally joined the IPTA, but they have been observer members with the intent to formally join at a later date and the MPTA has signed a data-sharing agreement with the IPTA already. In Russia, data from the Puschino Radio Astronomy Observatory were used for PTA-like experiments over ten years ago [38], but no results have been published recently. Finally, upgraded radio telescopes of the Argentine Institute of Radio Astronomy are also being used for MSP monitoring, with the ultimate aim to aid PTA studies [39,40]. A summary of the pulsars being monitored by the various PTAs can be found in Appendix A and a list of the various observatories involved in PTA experiments, along with some key properties of their observational data, is included in Appendix B.

[1] Many decades later it would be discovered that such black-widow systems can also be stable and some are presently being used in PTA experiments, see, *e.g.*, Bak Nielsen et al. [22],Desvignes et al. [23].

Steps in the PTA process

In essence, there are five steps in the scientific process of PTA research. First, pulsars are *observed*, typically at radio observatories [but see also 41]. The resulting data are written to disk for off-line processing. In the next step, which could be called "*basic timing*", these observational data get cleaned and reduced in order to ultimately convert the observations into a set of pulse ToAs and pulsar timing models. These timing models and ToAs are fed into the third stage (*noise modeling*), where the non-deterministic processes that affect the timing are determined. In an iterative way, this noise modeling further improves the timing model. In case of major changes to some of the parameters, some observations may need to be scrutinized in more detail or some part of the analysis may need to be re-done. The fourth step adds a further level of complication: in the "*GW Analysis*" step, the timing model is expanded to include correlated signals. At this step the data from all pulsars have to be simultaneously analyzed in a computationally-intensive Bayesian analysis that attempts to disentangle effects of the deterministic timing model, pulsar-specific noise parameters and correlated effects from clock errors, Solar-System ephemeris errors and GWs. Again, some iteration with the previous steps may be required. Finally, once the correlated signals are determined and the rest of the parameters have converged onto stable values, the final step of the *astrophysical interpretation* can be commenced.

In the following few sections, we will describe the various timing data sets that have been released, list the software packages that are typically used in these analyses, compare the noise modeling efforts of the major PTAs and discuss some of the more interesting sources of noise. After that, the recent GW analysis results and their astrophysical interpretations will be discussed.

PTA data sets

As discussed above, four PTAs (EPTA, InPTA, NANOGrav and PPTA) have joined forces within the IPTA. Beyond those the MPTA have released a data set and the CPTA have not yet released their data, but have published a description of their data set. The six most recently published data sets from these PTAs will be briefly described below and their main characteristics will be listed in Appendix B for the observational characteristics of the different PTAs and Appendix A for the list of pulsars monitored by the PTAs.

EPTA

The EPTA combines data from the five major radio astronomical telescopes in Europe: the Effelsberg 100-m radio telescope in Germany, the Nançay radio telescope in France, the Lovell telescope at Jodrell Bank Observatory in the UK, the Westerbork Synthesis Radio Telescope (WSRT) in the Netherlands and the Sardinia Radio Telescope (SRT) in Italy [23]. In addition, they coherently combine signals from these five radio telescopes to synthesize a continent-sized radio telescope with much higher sensitivity: the Large European Array for Pulsars [LEAP, 42], which was first included in the most recent analysis [43]. (Note that so far, SRT data have only been included in EPTA data sets as part of the LEAP data, but not as independent ToAs. Similarly, WSRT stopped providing independent ToAs in mid 2015 due to significant changes to the telescope receiver suite, after which it has only provided data that were merged into LEAP ToAs.) The low-frequency SKA pathfinder LOFAR [44] commenced a pulsar-monitoring campaign about a decade ago [45] and is expected to contribute to EPTA data sets in the near future [46]. Similarly, the French LOFAR extension NenuFAR [47] may contribute at even lower frequencies.

The EPTA has previously published data on 42 pulsars [23], but their most recent release only contained the 25 MSPs [43] that were expected to contribute the most GW sensitivity [48]. The timing programs at some of the EPTA observatories go back into the early 1990s, providing a full baseline of up to ~25 years, but their most constraining results were derived from the ~10-year long subset of data obtained with modern recording systems, although investigations into possible systematic effects or higher-level noise modeling for the earlier data may yet enable usage of the earlier data to further increase sensitivity. The variety of observatories contributing to this data set gives rise to a wide diversity of observing frequencies. The latest EPTA data release contained observations from 323 MHz at the low end up to 4.8 GHz at the upper end. Future inclusion of LOFAR data would push the lowest frequency down to ~100 MHz (inclusion of NenuFAR would bring the lowest frequency down below 100 MHz), while observations at the Effelsberg observatory may push the highest frequency up to 5 or even 9 GHz in future releases [49].

InPTA

The youngest of the IPTA's consortia published its first data release only recently [50]. It contains 14 MSPs and concentrates on low-frequency observations, varying from 300 MHz up to 1.46 GHz. The data set contains data from the recently upgraded GMRT and consequently is only 3.5 years long. Future additions of data from the Ooty Radio Telescope in Southern India may, however, be possible as well. Due to the low observing frequencies, the GMRT has concentrated primarily on mitigating interstellar propagation effects [35, see also Section "Current Challenges"] and teamed up with the EPTA's higher-frequency data set in order to derive GW results [43].

NANOGrav

The NANOGrav PTA has so far been dominated by the Arecibo and Green Bank radio telescopes [30], but the demise of the Arecibo 1000-foot telescope forced this PTA to look for other powerful telescopes to complement the GBT. In their most recent data release [51] they included pulsar-timing data from the VLA for the first time and a combination with data from the CHIME telescope is being prepared [52, 53].

The most recent data release from NANOGrav [51] contains nearly 16 years of data on 68 MSPs and has the widest persistent frequency coverage of any PTA, from 237 MHz up to 3 GHz.

PPTA

Formally the oldest PTA, the PPTA is centred around the 64-m Parkes radio telescope, Murriyang. Out of the four IPTA consortia it is the PTA with the smallest collecting area, but also the only one situated in the Southern hemisphere, providing it with the great advantage of being the only PTA with access to some excellent MSPs in the Southern sky. The third and latest PPTA data release [54] counted 32 MSPs with timing baselines up to 18 years. The PPTA originally used observations at three observing bands [29], with central frequencies around 700 MHz, 1.4 GHz, and 3.1 GHz, but in the last ~3 years started using an ultra-wide-bandwidth observing system that provides an instantaneous bandwidth from 704 MHz up to 4.032 GHz [55]. (Similar ultra-wide-bandwidth systems have been developed for the Effelsberg and Green Bank telescopes but those have not yet been included in PTA data releases so far.)

CPTA

The CPTA is not presently a member of the IPTA, but they coordinated their latest GW results to be released at the same time as those of the other PTAs [56]. While they have not actually released their data, the data that were used to obtain their GW result were obtained with the FAST radio telescope over the last 3.5 years over an observing bandwidth from 1 GHz up to 1.5 GHz. Their data set contains 57 MSPs.

MPTA

Finally, the MPTA carries out an MSP monitoring campaign with the SKA prototype telescope MeerKAT. Their first and latest data release contained 2.5 years of data on 78 MSPs across an observing bandwidth from 856 MHz to 1.712 GHz. The GW results from the MPTA's data have so far not been released.

Pulsar timing software

Observing software is typically specific to the data-taking system, although many recent systems employ either the DSPSR software package [57] or a system based on the CASPER platform [see, e.g., 58]. The observational data are most commonly stored in the PSRFITS format [59] and initial data reduction is typically carried out with the PSRCHIVE package [60].

A set of recommendations for pulsar timing practice and for metadata required in ToA files was presented in the appendix of Verbiest et al. [32] and a closer look at the algorithms used for ToA determination and template creation was recently published by Wang et al. [61] who experimentally confirmed some of the earlier recommendations.

For the analysis of the ToAs and the optimization of the timing models, the TEMPO2 package [62] is most commonly used outside North America, while the NANOGrav collaboration uses both the TEMPO2 and the independent, PYTHON-based PINT package [63], in order to allow independent verification of the timing results. The mathematical basis of the timing-model fit is fundamentally the same for the two packages and is detailed extensively by Edwards et al. [64].

For the noise modeling the NANOGrav and PPTA collaborations use the ENTERPRISE package [65], while the EPTA uses both ENTERPRISE and the slightly older TEMPONEST package [66]. The GW analysis is carried out with the ENTERPRISE package by all PTAs, although EPTA also uses the yet-unpublished "42" package.[2] The CPTA uses 42 for both noise modeling and GW analysis. Both ENTERPRISE and TEMPONEST are implementations of a Bayesian analysis code as described by Lentati et al. [66], but also contain modules with implementations of frequentist statistics for the GWB [30,67–69] and individual sources [70].

Most recently, the CEFFYL package [71] has been published, which aims to directly interpret PTA spectral data in terms of astrophysical models of the GWB in a computationally highly efficient way.

Noise analysis

As implied in our earlier discussion, there are four different types of signals that affect pulsar-timing data but are not included in the deterministic pulsar-timing model. Firstly, there is *white noise* which is expected to be quantified by the ToA uncertainties. However, these uncertainties are typically underestimated so that correction factors need to be defined [32]. Secondly, there is *achromatic red noise*,[3] which is commonly also referred to as *"timing noise"*, although the latter is also often used in a more generic context. Achromatic red noise is usually assumed to be related to intrinsic instabilities in the evolution of the pulsar's spin period, although no complete model has been proposed to date. It is known that this red noise in MSPs is typically at a lower amplitude than it is for slow pulsars [27,72] but the physical, underlying mechanism for this noise is not clear.

Achromatic red noise was first modeled in pulsar-timing efforts by Verbiest et al. [73] and their frequentist method was further expanded by Coles et al. [74]. In those early experiments the achromatic red noise was modeled with a broken power law since the assumption was made that the noise itself had a power-law shape [consistent with the findings in slow pulsars, 75] but that at the lowest frequencies this power would be absorbed by the fit for spin period and spindown. Presently, NANOGrav [76] as well as the EPTA [77] and InPTA [78] use power-law models for the achromatic red noise, while the PPTA uses a variety of noise models depending on the pulsar being studied [79,80, see below].

The third type of noise affecting pulsar-timing data, is *chromatic red noise*, which refers to non-deterministic variations in pulse arrival times which have some dependence on the observing frequency. The key difference with the achromatic red noise is that chromatic red noise could in principle be uniquely measured (and corrected for), provided observations at different observing frequencies are available. As discussed in Verbiest and Shaifullah [4], the fractional bandwidth of these multi-frequency data, as well as the sensitivity in the different bands, is key to such efforts, implying that ultra-wide observing systems (like the one used by the PPTA) or observations at very low frequencies (like those provided by the InPTA, LOFAR or CHIME) would provide the best chance at mitigation of this noise [see also 81]. Most PTA collaborations use a power-law model for each possible chromatic noise, while NANOGrav primarily uses the DMX model [82]. Efforts are ongoing to create more custom models for each pulsar based on the power-law model. Alternatively, as discussed by Janssen et al. [81], direct DM measurements at high cadence could also be used to correct higher-frequency data, as for example suggested by Donner et al. [46]. Yet another potential approach was put forward by Pennucci et al. [83], who developed software to simultaneously determine a DM value and a ToA from a given wide-band observation. This method is undergoing testing by NANOGrav, the InPTA and the PPTA. Specifically, NANOGrav has regularly published both traditional "narrow-band" ToA data sets and such experimental "wide-band" timing data [see, e.g., 51]. The InPTA's efforts are described by Paladi et al. [84] and the PPTA's analysis was recently published by Curyło et al. [85].

Chromatic red noise is generally caused by interactions between the radio waves and free electrons in the interstellar medium. Consequently the main component of such noise is temporal variations in interstellar dispersion, although higher-order terms caused by interstellar scattering that smears out the pulse profile shape [86] or frequency-dependent path-length differences [87,88] can also affect high-precision MSP timing data. A more extensive discussion of the various chromatic noise sources is presented in Section "Current Challenges".

The fourth and final type of noise affecting pulsar-timing data are sources of *correlated noise*, i.e. GWs and errors in clock standards and Solar-System ephemerides. These are also achromatic (i.e. independent of observing frequencies) but they have a well-defined correlation between pulsars, dependent on the angular separation on the sky between the pulsars in question.

PPTA

The most extensive noise models of any PTA were derived by the PPTA [79,80]. They analyzed all the types of noise described above, but more importantly, for the achromatic red noise, they developed different noise models for different observing bands or different observing systems,[4] as needed and included chromatic red noise with a variable spectral dependence. For ten (out of 26) pulsars they find that some band or system noise model is favored [79]. Nearly all their pulsars show evidence for dispersion measure variations (i.e. chromatic noise with a square-law dependence on the observing frequency) and

[2] Available from https://github.com/caballero-astro/fortytwo

[3] The combination "achromatic red" may appear confusing. Note that "achromatic" implies that this type of noise has no dependence on the *observing* frequency, whereas "red" refers to the fact that the power spectrum of this noise has excess power at low *Fourier* frequencies. In other words "achromatic red noise" is a type of noise that varies slowly in time but affects all photons in an identical way.

[4] Note this was also done for the first IPTA data release, [32,89].

for five pulsars they find chromatic noise with a different frequency dependence. Time-constrained, correlated and achromatic noise which they ascribe to temporary pulse-profile shape changes is detected in four pulsars. Such changes (see also Section "Profile-Shape Instabilities") have previously been detected in PSR J1713+0747 [23,82] and in PSR J1643−1224 [90].

The more recent PPTA work of Reardon et al. [80] further investigates the interplay between the noise models and sensitivity to potential GW signals. Specifically, they demonstrated that the choice of noise model significantly affects the evidence and recovered spectral properties of a common signal between the pulsars, underscoring the importance of detailed and well-informed noise-modeling in GW detection efforts.

NANOGrav

The NANOGrav collaboration's latest noise analysis [76] poses a stark contrast to the work of the PPTA in that they model the red noise only with a simple power-law model and demonstrate that this is sufficient to model their data in a statistically robust way. This was enabled using the DMX model [82] to describe the time variation of the dispersion measure as a series of fitted values between subsequent pairs of observations, where each pair consists of two observations within a few days at different radio frequencies. Assuming that the change of the interstellar medium within a few days can be neglected, one can fit for the offset caused by chromatic noise between the two observations in the pair.

They furthermore demonstrate that the MSPs in their sample can be divided into two groups: one group with strong red noise that appears to be pulsar-specific and a second group with lower-level red noise that appears to have identical spectral characteristics between the various pulsars observed [76, their Figure 2]. PSR J1939+2134 is the only source that does not match either group, as the spectral properties of its red noise falls in between the two groups.

InPTA

With only 3.5 years of data, the InPTA is not expected to be very sensitive to achromatic red noise, but given their low observing frequencies, variations in interstellar propagation delays (i.e. chromatic red noise) are a prime target of their observing strategy, as already pointed out in their earlier work on that topic [91]. The results from their full noise analysis were presented by Srivastava et al. [78] and confirmed that a majority of pulsars (8 out of 14) already showed significant chromatic noise, while four out of 14 even showed red noise that scaled more strongly with observing frequency than quadratic, which would be indicative of temporal variations in interstellar scattering – a clear demonstration of their high sensitivity to frequency-dependent propagation effects. Half of their pulsars (7/14) already showed signs of achromatic red noise, at levels that were consistent with results from the other PTAs.

EPTA/InPTA

The EPTA presented its latest noise analysis in a joint work with the InPTA [77]. They undertook a comprehensive comparison of the noise properties of various subsets of this combined data set, namely (a) the old EPTA timing data Caballero et al. [which effectively constituted the previously published results from 92], (b) the newer EPTA data and (c) the combined EPTA+InPTA data.

The findings were complex and highlighted the challenges of disentangling chromatic and achromatic red noise in data sets with lacking multi-frequency coverage. Specifically, the newer data set showed significant complications when compared to the earlier publication, largely due to two factors. First, the inclusion of the InPTA data significantly enhanced the sensitivity to chromatic red noise, but only during the few final years during which InPTA data were available; and second, the extremely long time baseline of the archival EPTA data provided significant sensitivity to any red-noise process, even if it did not allow discrimination between chromatic or achromatic noise. The inhomogeneous and time-variable nature of this combined data set provided complex results regarding the red noise, concluding that nearly a third of the pulsars studied (7 out of 25) required noise model that were more complex than a simple power law. For example, the red-noise properties of PSR J1713+0747 were found to not be stationary [which provides a fascinating point of comparison with the results presented by 80]. Additionally, tests for chromatic noise similar to [79] yield significant evidence for interstellar scattering in PSR J1600−3053. As a logical follow-up to these findings, efforts are now underway to combine the decade-long timing data from LOFAR [46] with the EPTA/InPTA data, in order to provide longer-term discrimination between different noise sources.

Unrelated to the main data-analysis efforts, Fumagalli et al. [93] also investigated the impact of outlier ToAs on PTA data analysis and PTA GW results, but concluded any impact would likely be negligible.

IPTA

A joint analysis of the data from the major PTAs is still under development, but a direct comparison of the noise models presented by the various PTAs was already published by Agazie et al. [94]. Notwithstanding the differences in the approaches of the various PTAs with regards to noise modeling, it was shown that there were no major inconsistencies between the PTAs' results and that any differences that did exist in the noise modeling were unlikely to affect searches for correlated signals between the pulsars of the various data sets.

Current challenges

In addition to red, frequency-dependent noise introduced by time-variable dispersion in the interstellar medium, a number of other effects can impact pulsar timing precision and have recently been studied in efforts to improve PTA sensitivity. In this section, we will review three such effects which are arguably the most relevant ones in present PTA analyses: profile-shape variations that were for several years considered to be "dispersion events" but have recently been shown to have a different origin, time-variable propagation delays introduced by the Solar Wind and possible consequences of interstellar scintillation.

Profile-shape instabilities

In recent years, several examples have been uncovered of temporary changes in the shape of MSP pulse profiles. These findings are of critical importance to any high-precision timing effort since the stability and reproducibility of the pulse profile is a fundamental assumption underpinning the technique. Originally, such changes were discovered in the timing of PSR J1713+0747 [23,30,82] and were thought to be due to transient events in the interstellar medium: minor gas clouds or bubbles that passed through the line of sight and temporarily changed the group velocity of the radio waves traveling to Earth [95].

A third such "event" that was observed in PSR J1713+0747 in 2021, however, was monitored more carefully than the previous two events and it was discovered that the cause of this event was by no means interstellar. Concerningly, the deviation in timing was shown to be caused by a temporary change in the pulse-profile shape of the pulsar [96–98]. A similar change was earlier seen in PSR J1643−1224 [90] and the PPTA claims to have detected similar behavior in PSRs J0437−4715 and J2145−0750 as well. These discomforting discoveries have raised awareness of the need to be on the look-out for instabilities in the pulse profile shapes, which has so far not been done routinely at any observatory.

The fact that these events affect the timing results is clear, but their impact on GW sensitivity is so far ill-defined. It is of note, however, that in their 12.5-yr analysis, NANOGrav pointed to these temporary events as one possible reason why PSR J1713+0747 was shown to contribute less than any other pulsar in their data set, to a red-noise signal of interest [99].

Solar wind

The Solar wind is a turbulent plasma that has a complex and rapidly varying distribution [100]. Furthermore, the lines of sight to pulsars pass through different parts of the heliosphere at different times of the year, causing the dispersive impacts on the pulse times of arrival to be highly variable throughout the year. In terms of how such variations impact PTA science, it is critical to bear in mind the difference between the additional delays experienced by the entire band (which is the actual impact on the timing and GW analyses) and the *difference* in dispersive delay measured across the observing band, as discussed in Verbiest and Shaifullah [4] (see, *e.g.*, their Figure 6).

For relatively high-frequency observations, or for observations with relatively limited fractional bandwidth, the differential delays *across* the band may be hard to determine, but the time variations affecting the entire band may still be highly significant — even if they cannot undeniably be identified as time-variable dispersive effects. As a consequence, studies of the Solar-wind impact on pulsar timing were hampered by the limited sensitivity of early data sets.

You et al. [101] were the first to attempt to determine the Solar-wind impact on PTA data and it was based on their partial success that subsequent PTA analyses [most explicitly 32] decided to remove all observations within five to ten degrees from the Sun, given the high likelihood of uncorrectable Solar-wind impacts. A dedicated analysis of the Solar wind effects on NANOGrav data was presented by Madison et al. [102], who did detect the Solar wind in some of their pulsars, but did not see any evidence of variations in the Solar-wind density on timescales of ~ 11 years, i.e. with the Solar cycle. These results stand in contrast with those from Tiburzi et al. [103], who used low-frequency LOFAR data to analyze the impact of Solar-wind variations in pulsar timing efforts and found clear evidence of Solar-cycle variability in the amplitude of the Solar-wind-induced delays, even if the significance of these variations was strongly dependent on the Solar latitude.

In a related publication, Tiburzi et al. [104] investigated how well analytic models were able to model the impact of the Solar wind on pulsar-timing data and found that none of the models commonly used by PTAs were sufficient to mitigate Solar-wind effects at levels required for GW science and that the remaining Solar-wind impact was significant far beyond the 5–10 degrees commonly excluded. Specifically, the authors argued that, unless significant progress is made in modeling Solar-wind impacts on pulsar timing data, all data within 20 (and in some cases even 40) degrees from the Sun may have to be considered corrupted.

Efforts to improve the negative impact of the Solar wind on PTA data are ongoing along three lines of research. First, phenomenological modeling of the Solar wind as part of the standard noise modeling has recently been developed and is starting to be used [105]. Second, combinations of PTA data with low-frequency data are being used to attempt a more precise modeling of both Solar-wind and interstellar propagation effects. Recent work by Niţu et al. [106] demonstrates that the traditional, high-frequency, PTA data are significantly affected by Solar-wind effects without being able to mitigate these effects, but that combination with low-frequency LOFAR data resolves this problem. Finally, interdisciplinary efforts at modeling the heliospheric electron density and space weather based on diverse data sets, to serve the dual purpose of solar astrophysics and PTA corrections for propagation effects, is being undertaken and has shown some promising preliminary results [107,108].

A less common impact from the Solar wind on pulsar timing would be the occurrence of coronal mass ejections (CMEs). These rapidly moving and relatively spatially constrained bullets of plasma occur regularly in the Solar System, particularly near Solar maximum. The chances of any single observation being affected by such an event are relatively minor, but given the size of PTA data sets and the fact that it can be extremely challenging to identify a single ToA that is offset, make it important to verify if no CMEs are affecting the PTA data. So far, only the InPTA has provided conclusive evidence of being affected by a CME [91], although it is likely other data have merely not been identified as being affected. Automated software to search for coincidences between PTA observations and CMEs has been made available in recent years by Shaifullah et al. [109].

Interstellar scintillation

The ionized plasma in interstellar space does not merely affect the light propagation time, but causes a host of more subtle effects as well. A group of related effects are often referred to as "scattering" or "scintillation", which depending on the context can be used interchangeably or as distinct observable effects. The physical mechanism that lies at the basis of both scattering and scintillation, is the fact that individual photons will take slightly different paths through interstellar space. Due to small-scale differences in the spatial distribution of free electrons, these different photons will arrive at the observer with slightly different phases, which causes interference and hence variations in observed brightness. Described in this way, the phenomenon is typically referred to as *scintillation* and it primarily affects the brightness of the pulsar observation [although higher-order effects are possible, see 4].

A different, but related, situation occurs when beams of radio waves are refracted in ways that cause their path-length differences to be significantly longer compared to waves that come along the shortest route. This would cause a significant spread in the arrival times of photons, depending on the path they traveled through interstellar space. The path-length differences are too significant to result in effective interference, but instead, the shape of the pulse profile will be smeared out, as a certain fraction of photons arrives with an appreciable delay. This phenomenon is often referred to as *scattering*. In itself such smearing of the pulse profile would only worsen timing precision, as it smooths over sharp features that enhance ToA precision, but in case the scattering is time-variable, this effect can also introduce significant noise in the timing data. Specifically, since the refraction angles are strongly frequency-dependent, such time-variable scattering effects would effectively introduce a chromatic type of red noise, which does not scale with the square of the observing frequency (like the dispersive propagation delays), but rather be an even stronger function of observing frequency.

For the following text, we will adhere to the definitions given above, namely that scintillation refers to minor refractive phase shifts that cause intensity interference at the observer's plane while scattering refers to larger-scale path-length variations that cause distortions in the pulse profile. However, the reader be warned that since both effects are fundamentally caused by refraction of the same interstellar, ionized plasma, many authors habitually refer to both effects as scattering.

Since scintillation does not in itself affect the pulse arrival time at a level that is commonly detectable at the timing precision that is typical of PTA data currently, it has so far not been considered a major complication for PTA research.[5] It has been used, however, as a complementary observable that can aid in defining accurate pulsar timing models for binary pulsars. This work was originally pioneered by Ord et al. [110] on PSR J1141−6545, but their analysis was corrected by

[5] In combination with profile evolution and excessively large ToA bandwidths, scintillation *can* cause issues, although in practice these are readily avoided, as described by Verbiest and Shaifullah [4].

Reardon et al. [111] who later also applied it to the PPTA pulsar J0437−4715 [112]. Similar work was done with PTA data specifically by Fonseca et al. [113], Perera et al. [33], Walker et al. [114], Askew et al. [115], Liu et al. [116], and Main et al. [117]. Of more direct relevance to PTA work, is the claim that scintillation information can be used to constrain (and potentially derive) variations in the density of free electrons, which causes the dispersive delays in the data. Initial results on this concept were recently published by Reardon and Coles [118] but have not yet been developed to the point where they can be practically applied to PTA data.

Scattering as defined above is of more direct consequence to PTA efforts since it directly affects the timing precision and if it is time-variable, it will be an additional source of red, chromatic, noise as well. To account for this in a phenomenological way, several PTAs have expanded their Bayesian noise-modeling efforts to include a chromatic red noise with variable power-law dependence on the observing frequency. Theoretically the strength of scattering is expected to scale with the observing frequency as $f^{-4.4}$, based on the assumption of thin-screen Kolmogorov turbulence [119]. Observational studies, however, have shown that this frequency dependence is in practice often a lot shallower [120] and can even be time-variable [121,122]. Furthermore, the frequency dependence of the scattering does not necessarily equate to the frequency dependence of the impact on the ToAs, since the way the ToAs are affected is most strongly influenced by the overall shape; and depending on specific features of the pulse profile, the impact on the ToAs may not scale as expected. Finally, the effective impact of the scattering on pulse profile shapes is usually assumed to be a convolution of the pulse profile with an exponential broadening function, based on the assumption of the scattering happening in an infinite, thin screen. This assumption has been shown to break down in a number of cases, either due to the limited size of the scattering screen [123] or due to high anisotropy in the scattering medium [124]. Both the PPTA [79] and the InPTA [78] have reported significant scattering variations in several pulsars; the EPTA has reported long-term scattering variations only in PSR J1600−3053 and NANOGrav did not see any evidence for scattering variations at all to date [76].

In principle the effects of scattering can be corrected through a process called *cyclic spectroscopy* [125], but this processing-intensive procedure must be ran on the raw data stream as it comes off the telescope and can hence not be applied retroactively on archival data. Some effort has gone into quantifying the potential benefit of such analyses, largely based on simulations. These investigations have demonstrated that for distant and strongly scattered pulsars, cyclic spectroscopy could significantly improve the timing quality and hence enlarge the number of MSPs that could meaningfully contribute to PTA efforts [126].

A final effect from the ionized component of the interstellar medium is effectively a combination of the effects we called scattering and scintillation earlier. As a basic explanation, consider two ray bundles that travel from the pulsar to the telescope, one along a mostly straight line and the other along a significantly longer path due to it being strongly refracted at one location along its travel path. Within each bundle of rays small-scale differences in phases will cause scintillation, but due to the long path difference between the two bundles, this scintillation pattern is modulated with a larger-scale interference effect, namely the interference between the two bundles, which works on larger scales.

In the frequency-time plane where scintillation is observable as random patches of intensity variations, this higher-order effect is seen as a corrugated modulation on top of those random patches. Taking the two-dimensional Fourier Transform of the intensities in the frequency-time plane returns the so-called *secondary spectrum* in which this modulated interference can readily be identified as parabolic distributions of power. This effect was first identified by Stinebring et al. [127] and it highlights the highly anisotropic nature of the ionized medium discussed above. In principle these *scintillation arcs* can be related to well-defined ionized structures in the ionized medium [see, e.g. 116], but in practice this may be sufficiently challenging [128] that using these structures for PTA corrections of interstellar propagation delays is still well beyond current capabilities. This phenomenon primarily gained interest after Hemberger and Stinebring [129] demonstrated that in some cases the refracted power from the secondary ray bundle could be sufficient to significantly affect the arrival times measured from the observed pulses. Consequently, a number of recent campaigns have tried to take stock of the prevalence of these arcs [128,130,131], but so far no significant effect on timing has been demonstrated beyond the work of Hemberger and Stinebring [129].

Signals and detections

PTAs are expected to detect mostly persistent signals in the form of a GW background and a number of individual binaries that are slowly evolving [132,133]. As a consequence, the GW signal builds up over time and with ever increasing instrumental sensitivity and longer observing timelines, a detection will slowly arise. This stands in sharp contrast to the GW detections made to date by the LIGO-Virgo interferometers, which have so far all been binary mergers that last much shorter than the observational timespan [134]. This causes a GW detection with PTAs to consist of three different stages: initially no signal will be detectable, so only limits can be placed on the amplitude of any GWs present in the data. At some point, these limits will saturate as the GWs start to significantly affect the timing of the most precisely timed pulsars. The first real (but ambiguous) signal that can be expected from GWs, is a ubiquitous red noise that equally affects all pulsars and that has common spectral characteristics in all pulsars — this type of signal is called “common red noise” (CRN) and would be the first indication of the presence of GWs [135]. A detection of CRN in itself is, however, not equal to a detection of GWs since the red noise could have a variety of origins and the consistency between pulsars may be coincidence or physical, but need not be due to GWs [136,137]. Therefore, the true detection of GWs can only occur when it is shown that the CRN is correlated between the pulsars in a quadrupolar way [8]. A detailed list of formal requirements to claim a statistically significant detection of GWs in PTA data was recently presented by Allen et al. [138]. Most importantly, they propose a 5-σ minimum statistical significance in order to differentiate a reliable detection from a chance alignment of noise.

Limits

The first limit on the amplitude of the Gravitational-Wave Background (GWB) after the formal commencement of PTA science was placed by the PPTA [139] and was about an order of magnitude higher than the most likely expected amplitude of an astrophysical GWB at the time [140,141]. Over the course of the decade that followed, PTA limits on the GWB amplitude got increasingly more constraining, down to the point where they were providing meaningful constraints on galaxy-evolution theory [142]. The most constraining limit to date is the one by Shannon et al. [142], which places a 95%-confidence upper limit on the dimensionless amplitude of the GWB of $A_{1\,\mathrm{yr}} < 1.0 \times 10^{-15}$ at a reference frequency of $1\,\mathrm{yr}^{-1}$, but some technical issues (detailed below) rendered this limit unreliable, so it was replaced with the slightly higher $A_{1\,\mathrm{yr}} < 1.2 \times 10^{-15}$ following a recent reanalysis [143]. This limit is closely followed by the most constraining limits from NANOGrav [$A_{1\,\mathrm{yr}} < 1.45 \times 10^{-15}$, 144], IPTA [$A_{1\,\mathrm{yr}} < 1.7 \times 10^{-15}$, 32] and EPTA [$A_{1\,\mathrm{yr}} < 3.0 \times 10^{-15}$, 145]. EPTA and PPTA did not publish a new limit after 2015, the IPTA only published a limit in 2016 and NANOGrav’s limit barely changed between 2016 and their last limit in 2018 (see Fig. 1). The lack of newly published limits was due to challenges the PTAs encountered in the form of red noise which saturated their ability to constrain the GWB further. This spurred an extensive push towards further improvements in data analysis and developments in

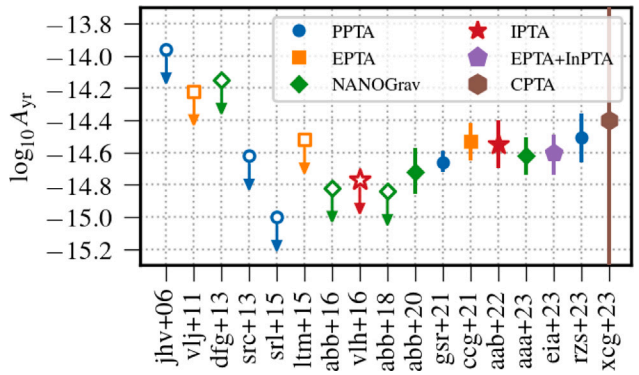

Fig. 1. Evolution of PTA sensitivity to gravitational waves. Shown are upper limits on the GW amplitude (unfilled markers with arrows) along with more recent measurements of CRN (first four filled markers with error bars from the left) and measurements of red noise with quadrupolar correlation between the pulsars (final four filled markers with error bars). Error bars are taken from the respective papers: NANOGrav, the EPTA, and the IPTA reported 90% confidence intervals while the PPTA reported 68% confidence intervals. Note that, due to reasons laid out in Section "Limits", some of the limits are unreliable and more constrictive than they really should be. The references given on the X-axis are: Demorest et al. [30],Verbiest et al. [32],Xu et al. [56],Arzoumanian et al. [99],Jenet et al. [139],Shannon et al. [142],Reardon et al. [143],Arzoumanian et al. [144],Lentati et al. [145],van Haasteren et al. [153],Shannon et al. [154],Arzoumanian et al. [155],Goncharov et al. [156],Chen et al. [157],Antoniadis et al. [158],Agazie et al. [159],Antoniadis et al. [160].

instrumental sensitivity and indicated a potential move towards an actual GWB detection soon.

During this time, there was significant interest in how errors in the Solar System ephemeris (SSE) would affect PTAs [136]. PTAs can be used to measure the masses of the planets [146] and search for unmodeled objects in the Solar System [12,147]. It was also noticed that PTA upper limits on the GWB amplitude were sensitive to the choice of SSE model used. Specifically, Arzoumanian et al. [144] demonstrated that the DE421 SSE model allowed much more stringent limits to be placed on the GWB amplitude than more recent, more accurate SSE models. Consequently, they proposed that some marginalization over some of the more ill-constrained parameters of the SSE model should be a key part of any PTA GW analysis. By adding those additional parameters to the analysis, limits would become more conservative and consequently more robust [see also the more detailed analyses by 14,148,149]. This joint analysis of GW signal and SSE model would allow a separation of the two signals and would therefore not only provide more robust limits, but also prevent false GW detections, as was pointed out earlier by Tiburzi et al. [136]. In practice, the corruptions of the DE421 ephemerides were largely alleviated by the inclusion of data from the Juno mission, which provided more accurate measurements of Jupiter's orbit [150].

In terms of interpreting upper limits on the GWB amplitude, Hazboun et al. [151] showed that Bayesian upper limits are sensitive to the choice of prior on the pulsar red noise due to the covariance between the two. Another potential issue with early upper limits is the number of pulsars used: Johnson et al. [152] showed through simulations that limits on the GWB may be biased if a small number of pulsars are used. This is an important factor to consider when interpreting early PTA upper limits since early PTA data sets included significantly fewer pulsars than are used currently. Due to these issues, some published limits on the GWB amplitude are likely unreliable and lower than they really should be.

Common red noise

Given the saturation of PTA limits, it was already clear that red noise was showing up. Whether this red noise had identical characteristics between the various pulsars was not clear until the work by Arzoumanian et al. [99], who published the first claim of "Common Red Noise" in their data, adding that this might be a suggestive first hint at actual GWs in their data. This work was soon followed up by confirmatory studies by PPTA [156], EPTA [157] and IPTA [158], all of whom confirmed a consistent signal with that presented by NANOGrav, but none of whom found significant evidence for interpulsar correlations. These results are summarized in Table 1 and Fig. 1.

Table 1
Summary of the amplitudes of CRN detections from the various PTAs, under the assumption of a spectral index of $\alpha = -2/3$, as expected from a GWB formed from SMBHB mergers.

PTA	$A_{\rm CRN}/10^{-15}$	Reference
NANOGrav	$1.92^{+0.75}_{-0.55}$	Arzoumanian et al. [99]
PPTA[a]	$2.2^{+0.4}_{-0.3}$	Goncharov et al. [156]
EPTA	$2.95^{+0.9}_{-0.7}$	Chen et al. [157]
IPTA	$2.8^{+1.2}_{-0.8}$	Antoniadis et al. [158]

[a] The PPTA reported a 1-σ uncertainty, whereas the other PTAs all reported 95% confidence intervals.

Extensive simulations were carried out to verify to what degree this CRN was a cause for excitement. Specifically, Goncharov et al. [156] did report on CRN in the PPTA data set, but also commented that this noise could be produced by noise inherent to the different pulsars and that there is evidence that it has to arise from a common process. This work was continued by Zic et al. [161] who carried out extensive simulations to show that CRN could easily be the result of a combination of pulsar-intrinsic timing noise with bad or inaccurate Bayesian priors. Nevertheless, Goncharov et al. [137] devised a method to differentiate between truly common red noise and merely 'similar' red noise, while finally proving that the red noise in the PPTA data was more likely to be truly CRN than merely a misidentification of spin noise. Similarly, the EPTA published an extensive analysis of their CRN signal [162], demonstrating that the characteristics of the signal were robust to significant changes in the noise modeling.

Hellings–downs correlation

The search for the tell-tale quadrupolar correlation signal in PTA data is more complex than it may seem on the surface. As early as 2016, Tiburzi et al. [136] warned of the potential corruption of different types of correlations: monopolar correlations introduced by clock errors and pseudo-dipolar correlations[6] caused by Solar-System ephemeris errors can readily be conflated in analyses that do not explicitly attempt to differentiate between the three types of correlations. Furthermore, the natural variance of the HD curve, and the use of a finite number of pulsars to measure the correlations complicate searches for the GWB [163–165]. A useful and accessible discussion of a variety of tricky aspects related to the quadrupolar correlation sought for in PTA data can be found in Romano and Allen [166].

With those caveats, PTAs searched their latest data sets and found for the first time evidence for correlations, building on the detections of CRN found in previous data sets that were discussed in the previous section. These results were published in a coordinated fashion on 29 June 2023 by the four PTAs that constitute the IPTA as well as the CPTA. Results are summarized in Table 2 and Fig. 1 and the relevant sensitivity curves are reproduced in Fig. 2. These results show that all the major PTAs have consistent results, albeit with variable sensitivity. NANOGrav obtained a 3-4-σ significance of a quadrupole-correlated signal [159], the EPTA achieved a ∼3-σ significance based on their most recent data combined with the InPTA's first data release [160]. The

[6] Correlations introduced by errors in the Solar-System ephemerides are strictly dipolar at any given point in time, but the direction of the dipole slowly moves on the sky, causing the actual effect in a long-term data set to be more complex than a straightforward dipolar correlation.

Table 2
Summary of GWB results from the PPTA, EPTA+InPTA, CPTA, and NANOGrav. The GWB can be described in terms of the characteristic strain spectrum $h_c(f) = A_{\rm yr}(f/f_{\rm yr})^{\alpha}$ or the residual power spectral density $P(f) = h_c(f)^2/(12\pi^2 f^3) = A_{\rm yr}^2/(12\pi^2)(f/f_{\rm yr})^{-\gamma}\,{\rm yr}^{-3}$, where $\gamma = 3-2\alpha$. Quoted are 90% credible intervals, except for the PPTA, where the 68% confidence interval is given.

PTA	$\log_{10} A_{\rm yr}$	γ	Reference
EPTA+InPTA[a]	$-14.10^{+0.25}_{-0.44}$	$3.03^{+1.02}_{-0.67}$	eia+23b
NANOGrav	$-14.19^{+0.22}_{-0.24}$	3.2 ± 0.6	aaa+23c
CPTA[b]	$-14.4^{+1.0}_{-2.8}$	[0, 6.6]	xcg+23
PPTA	$-14.50^{+0.14}_{-0.16}$	3.87 ± 0.36	rzs+23b

[a] For the EPTA/InPTA combination the results from their DR2new+ data set are shown.
[b] Note the CPTA reported their results as constraints on the characteristic strain spectrum, with $\alpha \in [-1.8, 1.5]$. The references given, are: Antoniadis et al. [160], Agazie et al. [159], Xu et al. [56] and Reardon et al. [143].

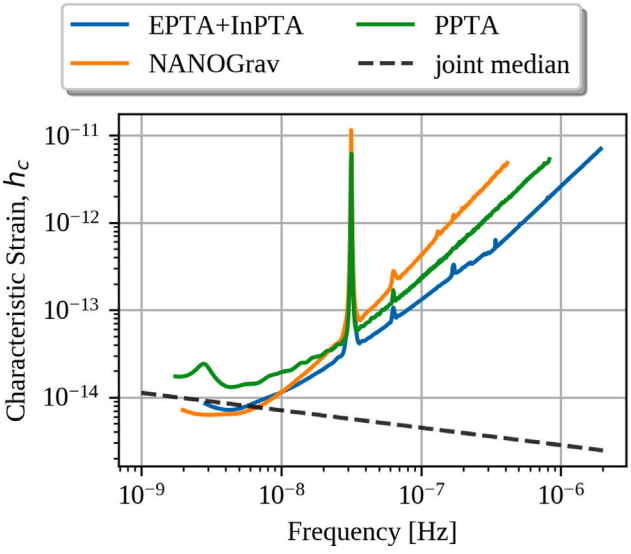

Fig. 2. Sensitivity to a GWB for the four main PTA collaborations. Shown are the sensitivity curves for the most recently published GWB analyses of the four main PTA collaborations [143,159,160], where EPTA and InPTA provided a joint analysis. The dashed line shows the best-fit GWB spectrum based on the joint probability distribution of the three publications.
Source: Reproduced from Agazie et al. [94].

PPTA obtained a ∼2-σ result but note that the signal they detect is not stationary: in the earlier part of their data the amplitude they detect is different [143]. Finally, the CPTA presented a ∼4.6-σ result for GWs at the frequency of 14 nHz [56], but since their analysis is fundamentally different from the analyses of the other PTAs; and since their data have so far not been publicly released (in contrast to the data from the other PTAs), it is presently impossible to meaningfully compare this value to the levels of detection significance from the other PTAs.

None of the PTAs reached the 5-σ level of significance required according to Allen et al. [138], so that formally none of the PTAs have been able to claim a statistically significant *detection* of GWs in the nHz band, meaning that the measured correlations can merely be seen as *evidence for* GWs in the PTA data. Hopes are that the addition of more recent data and the combination of data from all the various PTAs would push the significance levels to beyond the 5-σ level, although these efforts are still ongoing. Also the high sensitivity of the CPTA data, following a very brief observing campaign, raises hopes for the MPTA data set which has yet to announce its GW results.

Individual supermassive binary black holes

While the preceding sections focused on a broadband spectrum of GWs produced by a stochastic GWB, an alternative source of GWs would be individual supermassive binary black holes which would emit GWs at a single frequency provided they are in circular orbits that do not evolve over the time span of the observational campaign.

Perera et al. [167] used a dedicated high-cadence data set on PSR J1713+0747 to constrain single sources of GWs at the highest GW frequencies accessible to PTAs, deriving $A_{1\,\mu Hz} < 3.5 \times 10^{-13}$ for the sky-averaged limit on the amplitude of individual GW sources at a GW frequency of 1 μHz, which equates to periods of about two weeks. Efforts have also been undertaken to use PTA data sets to detect GWs from a single binary. Falxa et al. [168] analyzed the second data release of the IPTA [33] for continuous GWs and derived a 95% upper limit on the gravitational strain of these binaries between 10^{-13} and 10^{-14}, depending on the exact frequency, with optimal frequency around 10 nHz. No significant signals were found.

More recently, searches were undertaken by the EPTA/InPTA [169] and NANOGrav [170] collaborations. EPTA/InPTA and NANOGrav both found weak evidence for a signal near 4 nHz, but both studies concluded this signal was lacking statistical significance and did not provide sufficient evidence for quadrupolar correlations. Antoniadis et al. [169] concluded their 4–5 nHz "signal" could be a misinterpretation of a GWB signal and pointed out data sets with more sensitivity would be needed to enable a decisive conclusion. Agazie et al. [170] furthermore found some weak evidence for a feature at 170 nHz but decided this was also unlikely to be a real GW source given the high GW frequency and the fact that the signal seemed dominated by a single pulsar which has an orbit with a similar period as that of the candidate GW signal.

While the majority of searches for GWs from individual binaries have assumed circular orbits, some binaries emitting GWs at nanohertz frequencies may have significant eccentricities. These searches are more computationally intensive and require more complex signal models [171–173]. Agazie et al. [174] used the most recent NANOGrav data set to perform a search for GWs from an eccentric binary at a particular SMBHB candidate, 3C66B [175]. They derived an upper limit on the chirp mass of $(1.98 \pm 0.05) \times 10^9\,{\rm M}_\odot$ (95% confidence) for orbital eccentricities lower than 0.5 and a symmetric mass ratio above 0.1.

To conclude our discussion of individual SMBHB sources, we point out that many of the potential pitfalls that made early GWB limits unreliable (such as inappropriate priors, inaccurate SSE models, possible bias in pulsar selections and excessive or lacking modeling of intrinsic pulsar noise) can also affect limits on individual GW sources. Increasing awareness does imply any such effects are likely to be less prominent in more recent analyses, however.

Anisotropy in the background

In between the extreme scenarios of a GWB and an individual GW source, is an anisotropic background of GWs. This is essentially a combination of a GWB with several bright GW sources that stand out beyond the background. In such a scenario the overall anisotropic character of the GWB would be identifiable before any individual source would be confidently detectable [see, e.g., 176,177]. According to the work by Pol et al. [178], a 20-year data set with characteristics similar to those of the NANOGrav PTA, would have a realistic chance of detecting anistropy at the 3-σ level. This work is based on the assumption that the GW signal strength scales with $\sqrt{N_{\rm psr}\left(N_{\rm psr}-1\right)/2}$ (where $N_{\rm psr}$ is the number of pulsars in the array), which explains why NANOGrav is predicted to have the best chance of detecting such a GWB, given that it has the largest number of pulsars in its array. However, this scaling law [taken from 179] implicitly assumes all pulsars are in the "strong-signal" regime and contribute equally — which is likely not the case in any realistic PTA. Also, this predictive

work assumed an anisotropy level[7] of $C_{l=1}/C_{l=0} = 30\%$, but the latest work by Agazie et al. [180] already constrained the GWB anisotropy below this level: $C_{l=1}/C_{l=0} < 27\%$.

Astrophysical interpretation

Generally the most likely source of GWs in the PTA band is considered to be supermassive black-hole binaries (SMBHBs) that are the consequence of hierarchical galaxy evolution. In this case, two different types of GWs could be detectable by PTAs: the purely stochastic GWB that would be characterized by a red-noise spectrum, or individual SMBHB sources that would be monochromatic and unevolving within our lifetime. It is considered increasingly likely that a combination of these sources would be detected — or an early indication of such a combination, i.e. a GWB with anisotropic features. Notwithstanding the focus that has been placed on SMBHBs, a diverse range of alternative sources of GWs has also been proposed, most commonly related to strings or inflation. Alternatively, the PTA data can also be used to detect or place constraints on GW polarization or on ultra-light dark matter (ULDM), which is expected to result in monopolar rather than quadrupolar correlations.

In this section, we will briefly review some of the main research that has been recently derived on these sources based on the most recent PTA results.

Supermassive binary black holes

A good review on the basics of SMBHBs and how they can be detected through GWs, is given by D'Orazio and Charisi [181]. Fundamentally, as galaxies merge, the supermassive black holes at their centers form binaries that ultimately lead to mergers. Such a SMBHB emits gravitational waves with a GW frequency twice the orbital frequency and can hence be detectable in PTA data for orbital periods in the range of years to decades. Since most of these binaries are expected to be relatively distant and faint, they may not be easily detected individually, but their combined stochastic sum is expected to reach a level that should soon be detectable by PTAs.

Based on the signals reported in Section "Hellings-Downs Correlation", both NANOGrav [182] and EPTA/InPTA [183] have studied the implications of this signal for SMBHB models. Both groups found that many different models for galaxy evolution and SMBHB formation and evolution are technically statistically consistent with the data, but that typically either many parameters are on the edge of their predicted ranges, or that a few parameters are significantly inconsistent with expectations. Specifically, Antoniadis et al. [183] point out – based on the results from L-galaxies simulations [184,185] – that the high amplitude of the signal implies a shorter SMBHB evolutionary timescale and, more importantly, a higher gas accretion rate than usually expected, but that this may cause tension with other observables like the AGN luminosity function. Furthermore, the fact that the spectral slope is shallower than expected may be interpreted as an indication that the GWB is not dominated by circular SMBHBs, but that eccentric SMBHBs or other environmental effects play a significant role as well, or that small-number statistics may be at play (in which case a detection of anisotropy in the background should be expected in the near future).

The methodology behind these analyses was studied by Valtolina et al. [186] who found that the results were mostly robust, provided care was taken with the assumed GWB models. In particular astrophysical results referring to SMBHBs could be significantly biased depending on the chosen GWB models. Essentially these conclusions are consistent with the model-dependent results presented by Agazie et al. [182] and Antoniadis et al. [183].

It is worth noting that the GW analyses carried out by the PTAs makes several simplifying assumptions about the GWB (Gaussianity, isotropy, and often a power-law spectrum), none of which are exactly satisfied by a GWB produced by a finite number of supermassive binary black holes. Bécsy et al. [187] studied the impact of these assumptions by generating simulated data sets with astrophysically realistic GWB and using standard methods to recover their properties. They found that the analyses were robust and able to detect the GWB with these simplifying assumptions, although there was a large variance in the significance and recovered parameters.

Early universe: Inflation and strings

A number of different mechanisms (many of which relate to cosmic strings) can create a GWB at the earliest times of the Universe's evolution, as reviewed recently by Lino dos Santos and van Manen [188]. Under the assumption that the signals described in Section "Hellings-Downs Correlation" arise from that era, these theoretical predictions can be tested. Based on the most recent NANOGrav results, Afzal et al. [189] investigated the consistency of the observations with various cosmological interpretations, namely inflation, scalar-induced GWs, first-order phase transitions, cosmic strings and domain walls. They find that when performing a simple phenomenological fit to the observed power spectrum of the common signal most cosmological models provide a better match to the data than the GWB from SMBHBs does, with the exception of one model which they rule out, the stable cosmic strings that have a field-theory origin. However, the reader should be cautioned that the attained evidence for various models explaining the observed signal is very weak and is expected to change as more realistic simulations of the SMBHB background and improved noise models are incorporated in the analysis. Antoniadis et al. [183] analyzed the EPTA/InPTA results and come to an overall similar conclusion: both astrophysical and cosmological models can explain the data equally well. Though, one should point out that for most of the signals of cosmological origin the obtained best-fit parameters would be challenging to interpret in the frame of standard inflation. A similar conclusion based on the NANOGrav results is reached by Vagnozzi [190] who points out that an "extremely blue tensor spectrum" would be required to make the observations consistent with an inflationary origin. After analyzing a wide variety of early-universe models, Vagnozzi [190] concludes that the ekpyrotic model of the early universe [191] appears the most natural fit to the data, even though these models are typically expected to generate a GWB with a significantly lower amplitude than the one observed in PTA data.

Ultra-light dark matter

A number of different models have been proposed that predict an impact of ULDM on PTA data. Specifically, Khmelnitsky and Rubakov [192] developed a description in which ULDM interacts with normal matter purely gravitationally. This would introduce oscillating gravitational potentials which would affect the propagation of photons through space and hence affect pulsar timing results. This model was the basis for the limits placed by Porayko et al. [193], based on PPTA data. They improved previously derived limits by a factor of two to five, resulting in a limit on the dark-matter density of ultralight bosons of: $\rho < 6\,\mathrm{GeV/cm^3}$ at 95% confidence in the mass range $m \leq 10^{-23}$ eV. A more constraining result in a slightly more restricted mass range was recently placed by Smarra et al. [194] based on the EPTA data: $\rho \leq 0.3\,\mathrm{GeV/cm^3}$ in the mass range $10^{-24}\,\mathrm{eV} \leq m \leq 10^{-23.4}\,\mathrm{eV}$, implying that fuzzy dark matter in this mass range is disfavored by pulsar timing data. The constraints found by Afzal et al. [189] are very comparable: $\rho \leq 0.4\,\mathrm{GeV/cm^3}$ for $m \leq 10^{-23}\,\mathrm{eV}$.

[7] The anisotropy level is quantified as a ratio of the squared angular power C at angles of 180° ($l = 1$) to the squared angular power in the multipole mode ($l = 0$). A fully isotropic background would only have power in the multipole mode, reducing the ratio to 0, whereas an anisotropic background would have power at the higher modes as well, creating a positive value for the ratio $C_{l=1}/C_{l=0}$.

Independently, Afzal et al. [189] used the most recent NANOGrav data to place a limit on ULDM interacting with the particles of the standard model. While the physical mechanisms for how the ULDM affects pulsar timing measurements differ greatly between the two cases, the observational effects are ultimately highly similar. Specifically, Kaplan et al. [195] do not consider gravitational interaction, but instead consider the case in which ULDM is directly coupled to standard matter through QED or QCD sectors, which causes variations in the moment of inertia of pulsars or shifts in the terrestrial atomic time standards, which affects the pulsar timing results. In particular, the effect of the latter shows a strictly monopolar correlation between the residuals of different pulsars. Additionally, the background of coupled vector ULDM particles can induce dark "electric" fields, which cause periodic displacements between the Earth and any given pulsar [196,197]. Through these mechanisms, Afzal et al. [189] set stringent upper limits on the coupling constant between ULDM and standard model particles which are competitive with (and in some cases outperform) laboratory constraints in the mass range $10^{-24}\,\mathrm{eV} \leq m \leq 10^{-20}\,\mathrm{eV}$ [198–200].

Alternative polarization modes

Studying the polarization modes of gravitational waves with LIGO-Virgo-KAGRA (LVK) detectors is challenging due to the small number of interferometer arms to date, the short duration of most detected signals and the fact that the design of the LVK detectors is tuned to standard polarization modes predicted by general relativity [201,202]. It is possible, though, to put stringent constraints on the presence of alternative polarizations using the current network of detectors [203,204]. The limits can be further improved in the presence of an identifiable electromagnetic counterpart [201] or through observation of strongly lensed GW signals [205]. However, in order to fully characterize all six distinct polarization modes that are predicted by alternative theories of gravity, one needs six linearly independent GW detectors [206]. For PTAs, the situation is drastically different, primarily due to the large number of Earth-pulsar detection "arms" and there are realistic prospects to probe the polarization of GWs [207,208]. Efforts to place constraints on GW polarization modes were recently undertaken by Wu et al. [209],Agazie et al. [210], but so far no distinction can be made between the standard and alternative gravity theories.

Anticipated improvements

The scaling laws for PTA sensitivity to a GWB depend on a number of factors related to the PTA's design and to the detection regime the PTA is in. Since it appears PTAs are approaching a detection, typically the scaling law is presumed to be the following [179,211]:

$$S/N \propto N\sqrt{T}\left(\frac{A\sqrt{C}}{\sigma}\right)^{3/13}, \tag{1}$$

where S/N is the signal-to-noise ratio of the GWB in the data, N is the number of pulsars in the array, T is the timing baseline of the PTA data set, A is the dimensionless amplitude of the GWB at the reference frequency of $1\,\mathrm{yr}^{-1}$, C is the cadence of the observations and σ is the level of the timing precision, typically taken to be the weighted RMS of the timing residuals. This equation provides a number of clear paths forward to effectively boost the sensitivity of PTAs to a GWB.

International collaboration. The foundation of the IPTA in 2008 [31] was a logical step towards developing PTA sensitivity, since global combination would immediately increase N (as all-sky access becomes possible with telescopes in both hemispheres) and C. While this appears straightforward on paper, the IPTA data combinations turned out to be more complicated than anticipated, although an improvement in GWB sensitivity by a factor of at least two was demonstrated [32]. Given the recent results from constituent PTAs, it is anticipated that the next IPTA data combination [212] may provide the first GWB detection with a significance beyond 5 σ.

Continued observations. In the low-S/N regime, PTA sensitivity scales with $T^{13/3}$ and hence GWB limits increase rapidly [179]. However, as we approach a detection, a transition occurs and detection significance only increases slowly with observing timespan, i.e. with $T^{1/2}$. Due to the complexities inherent to long data sets [see, e.g., 43], which have additional impacts from timing noise and interstellar dispersion variations, and which often suffer from inhomogeneities due to changes in instrumentation, longer timespans in the detection era may provide more challenges than benefits. This is underscored by the power of highly sensitive telescopes like MeerKAT and FAST, which have PTAs with short timing baselines which are still competitive with the older PTAs that have far longer timespans [37,56].

New telescopes. As hinted in the previous paragraph, new, more powerful telescopes like the MeerKAT telescope array or the Chinese FAST telescope, can significantly improve the timing precision of MSPs by beating down the white noise. A case in point provides the timing of PSR J1933−6211, which was timed by both the Parkes telescope [213] and MeerKAT [214] in recent years. The enhanced timing precision provided by MeerKAT enables a lot more science with a lot less complications [see, e.g., 215]. The same conclusion is likely to hold true for PTA research. In addition to MeerKAT [216] and FAST [217], in North America the Deep Synoptic Array [DSA-2000, 218] has PTA science as its third key science objective and is planning to allocate 25% of its observing time to it. Finally, construction has commenced on the Square Kilometre Array (SKA) telescope, which is also expected to host a high-impact PTA program [81].

Wide-band receivers. A major change in the sensitivity of pulsar timing experiments over the past several decades, has been the development of wide-band receiver systems. The PPTA has commenced PTA observations with such a system [85], having a bandwidth from 704 MHz up to 4.032 GHz [55]. The key advantages of such systems for PTA work are an increase in sensitivity (lowering σ) but also additional sensitivity to frequency-dependent effects, which may aid noise-modeling and thereby increase sensitivity. Similar plans for wide-band receivers have been developed for the GBT and the Effelsberg radio telescopes, although PTA observations with those systems have so far not been published.

Diverse PTAs. So far, most PTAs have concentrated their observing campaigns on the GHz frequency range. With the upcoming addition of the low-frequency LOFAR [46], NenuFAR [47] and CHIME [52] radio telescopes, data with additional sensitivity to propagation effects and with higher cadence will become possible. Furthermore, the recently proposed Gamma-ray PTA [41] will complement these efforts by providing a timing baseline that is fully unaffected by interstellar propagation effects.

More pulsars. As can be seen in Fig. 3, even though the pulsar surveys from the mid-1990s and early 2000s were considered sufficiently successful to warrant the commencement of PTA experiments, discovery rates in recent times have consistently been higher than back then. This bodes well for PTA experiments, not only because the number of MSPs in PTAs can be continuously increased, thereby enhancing sensitivity to GWs, but also because the best MSPs can be selected from an ever-growing population. However, part of the reason that so many new MSPs are being discovered in recent times, is that observing hardware has been upgraded, thereby allowing fainter sources to be discovered. As shown in Fig. 4, the average flux density of discovered disk MSPs has persistently decreased, implying that any newly discovered MSP is fainter and hence on average less useful for high-precision timing efforts. This trend is clearly partly counter-acted by the increased sensitivity of observing systems and new telescopes, but does clarify an increased reliance on that additional sensitivity. (We restricted ourselves to disk MSPs, which were defined as pulsars with spin periods shorter than 30 ms and spin-down rate below 10^{-15} s/s and which are

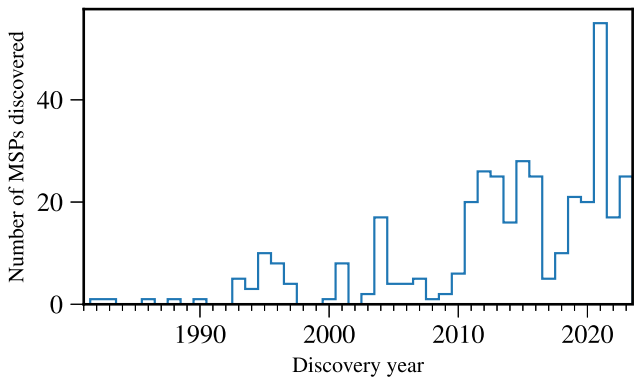

Fig. 3. Number of Galactic disk MSPs discovered as a function of time. Primarily due to the surveys with a new generation of highly sensitive telescopes (FAST, MeerKAT), the discovery rate in recent years has remained as high as it has ever been. Data from the ATNF pulsar catalog, version 2.1.0 [219]. Note that a more up-to-date list of MSP discoveries is maintained at https://www.astro.umd.edu/~eferrara/pulsars/GalacticMSPs.txt, which presently contains 49 more unpublished MSPs, primarily discovered in the last ~ 5 years. For the purpose of this plot, however, we chose to only display published pulsar discoveries.

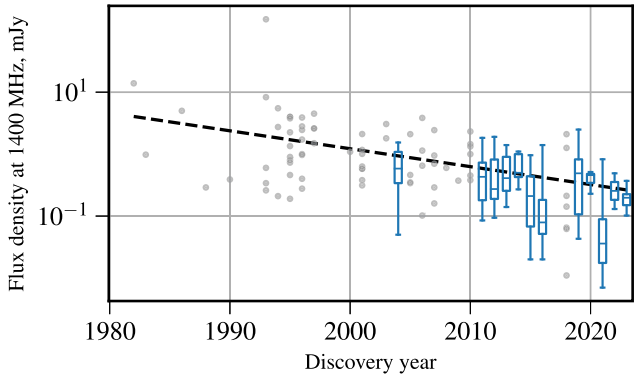

Fig. 4. Flux density at 1.4 GHz observing frequency of disk MSPs as a function of discovery year. In years where more than 15 data points are available, box plots are shown instead of the individual measurements. The box plots show the median as a horizontal line, the 25-75th percentiles as a box and the extreme values as whiskers. As expected for ever more complex and ever deeper surveys, the brightness of newly discovered MSPs has consistently trended downwards.(Data from ATNF catalogue version 2.1.0, Manchester et al. [219]).

not associated with globular clusters. While many MSPs inhabit globular clusters, due to the high density in the cluster environment, these MSPs undergo unpredictable accelerations that add strong red noise in their timing, thereby making their inclusion in PTAs particularly problematic.)

Novel analysis methods. The primary challenge in current PTA analyses is the computational load and processing time, particularly for the Bayesian GW analysis and noise modeling. Consequently, research is being undertaken along multiple lines to attempt and improve the processing speed, for example by optimizing Bayesian samplers [220], or by applying artificial intelligence methods [221]. Since both noise modeling and GW analysis typically rely on spectral analysis, optimized routines for spectral characterization have also recently been proposed by Lamb et al. [71]. (Note that the uneven sampling of PTA data sets is usually not a problem since the analysis routines Fourier-transform the models rather than the data.)

Discussion and conclusions

PTAs hold the prospect of detecting GWs from a diversity of sources, although most commonly they are expected to probe a GWB created by multitudes of SMBHBs distributed throughout the Universe. In recent years, multiple indications have been presented that make a convincing case supporting the expectation that a full detection of GWs by PTAs is imminent. This would open the nHz-frequency part of the GW spectrum and provide GW observations that are highly complementary to those provided by the LIGO/Virgo/KAGRA collaboration. PTAs are accelerating their progress towards detection through a diverse combination of efforts, not in the least through international collaboration, but also through continued hardware improvements and improvements in data-analysis techniques and by adding complementary observations to their analyses. Limits and preliminary results that hint at a future detection are already being used to constrain a diverse set of cosmological, gravitational and astrophysical models for GWBs and while the results are generally not fully consistent with standard model predictions, preferred models can still be tuned to match observations. This suggests that even the first 5-σ detection may already provide significant astrophysical insights in processes that have so far been the monopoly of N-body simulations.

CRediT authorship contribution statement

Joris P.W. Verbiest: Writing – review & editing, Writing – original draft, Visualization, Validation, Supervision, Project administration, Methodology, Investigation, Conceptualization. **Sarah J. Vigeland:** Writing – review & editing, Visualization, Validation, Methodology, Investigation. **Nataliya K. Porayko:** Writing – review & editing, Visualization, Validation, Investigation, Conceptualization. **Siyuan Chen:** Writing – review & editing, Validation, Methodology. **Daniel J. Reardon:** Writing – review & editing, Validation.

Declaration of competing interest

The authors declare that they have no known competing financial interests or personal relationships that could have appeared to influence the work reported in this paper.

Data availability

No data was used for the research described in the article.

Acknowledgments

The authors wish to express their gratitude to the lively, passionate and highly diverse community that drives the exciting research summarized in this paper. We are particularly grateful to the technical staff and operators at the many radio telescopes across the world, who keep their instruments in top shape and continue to provide the highest quality data that are required for the GW detection we are all jointly moving towards. The authors particularly wish to thank the two referees and the following colleagues: Maura McLaughlin, Golam Shaifullah, Deborah Good, Boris Goncharov, Michael Lam, Krishnakumar M. A., William Lamb, Jackson Taylor and Jeremy Baier for useful discussions, comments and suggestions, which have significantly improved this paper. JPWV acknowledges support through the Space Research Initiative, USA (SRI, award number AWD00005725), managed by the Florida Space Institute (FSI) and from National Science Foundation (NSF) AccelNet, USA award No. 2114721. SJV acknowledges support from NSF, USA award No. 2309246 and NSF Physics Frontiers Center, USA award No. 2020265. NKP funded by the Deutsche Forschungsgemeinschaft (DFG, German Research Foundation) – Projektnummer PO 2758/1–1, through the Walter–Benjamin programme. Parts of this research were conducted by the Australian Research Council Centre of Excellence for Gravitational Wave Discovery (OzGrav), through project number CE170100004.

Table A.3
MSPs that are being timed as part of a PTA experiment. Listed are the J2000 name of the pulsar, its pulse period, interstellar dispersion measure, orbital period (if any), measured flux density at 1.4 GHz and which PTAs it is observed by ('V' indicates the pulsar is part of the array, '-' indicates it is not). Values were taken from the ATNF Pulsar Catalogue [219], Agazie et al. [51] or from Fiore et al. [222] in the case of PSR J1327+3423. The source lists from the various observing campaigns were taken from the references cited in Section h.

Name	Period	DM	P_b	S_{1400}	Observed by						
(J2000)	(ms)	(pc/cm^3)	(days)	(mJy)	EPTA	InPTA	NANOGrav	PPTA	CPTA	MPTA	LOFAR
J0023+0923	3.05	14.3	0.1	0.7	–	–	V	–	V	–	–
J0030+0451	4.87	4.3	–	1.1	V	–	V	V	V	V	V
J0034−0534	1.88	13.8	1.6	0.2	–	–	–	–	V	–	V
J0125−2327	3.68	9.6	–	2.5	–	–	–	V	–	V	–
J0154+1833	2.37	19.8	–	0.1	–	–	–	–	V	–	–
J0218+4232	2.32	61.3	2.0	0.9	–	–	–	–	V	–	V
J0340+4130	3.30	49.6	–	0.3	–	–	V	–	V	–	–
J0406+3039	2.61	49.4	7.0	–	–	–	V	–	V	–	–
J0407+1607	25.70	35.6	669.1	0.4	–	–	–	–	–	–	V
J0437−4715	5.76	2.6	5.7	150.2	–	V	V	V	–	V	–
J0509+0856	4.06	38.3	4.9	1.5	–	–	V	–	V	–	–
J0557+1551	2.56	102.6	4.8	–	–	–	V	–	–	–	–
J0605+3757	2.73	20.9	55.7	–	–	–	V	–	V	–	–
J0610−2100	3.86	60.7	0.3	0.7	–	–	V	–	–	V	–
J0613−0200	3.06	38.8	1.2	2.3	V	V	V	V	V	V	–
J0614−3329	3.15	37.1	53.6	0.7	–	–	V	V	–	V	–
J0621+1002	28.85	36.6	8.3	1.7	–	–	–	–	V	–	V
J0636−3044	3.95	15.5	–	1.5	–	–	–	–	–	V	–
J0636+5128	2.87	11.1	0.1	1.0	–	–	V	–	V	–	–
J0645+5158	8.85	18.2	–	0.3	–	–	V	–	V	–	V
J0709+0458	34.43	44.3	4.4	0.3	–	–	V	–	–	–	–
J0711−6830	5.49	18.4	–	2.6	–	–	–	V	–	V	–
J0732+2314	4.09	44.7	30.2	0.7	–	–	–	–	V	–	–
J0740+6620	2.89	15.0	4.8	1.1	–	–	V	–	–	–	V
J0751+1807	3.48	30.2	0.3	1.4	V	V	–	–	V	–	V
J0824+0028	9.86	34.5	23.2	0.5	–	–	–	–	V	–	–
J0900−3144	11.11	75.7	18.7	3.8	V	–	–	V	–	V	–
J0931−1902	4.64	41.5	–	0.5	–	–	V	–	–	V	–
J0952−0607	1.41	22.4	0.3	–	–	–	–	–	–	–	V
J0955−6150	2.00	160.9	24.6	0.6	–	–	–	–	–	V	–
J1012−4235	3.10	71.7	38.0	0.3	–	–	V	–	–	V	–
J1012+5307	5.26	9.0	0.6	3.8	V	V	V	–	V	–	V
J1017−7156	2.34	94.2	6.5	1.1	–	–	–	V	–	V	–
J1022+1001	16.45	10.3	7.8	3.9	V	V	V	V	–	V	V
J1024−0719	5.16	6.5	–	1.5	V	–	V	V	V	V	V
J1036−8317	3.41	27.1	0.3	0.5	–	–	–	–	–	V	–
J1045−4509	7.47	58.1	4.1	2.7	–	–	–	V	–	V	–
J1101−6424	5.11	207.4	9.6	0.3	–	–	–	–	–	V	–
J1103−5403	3.39	103.9	–	0.4	–	–	–	–	–	V	–
J1125−5825	3.10	124.8	76.4	1.0	–	–	–	–	–	V	–
J1125−6014	2.63	52.9	8.8	1.3	–	–	–	V	–	V	–
J1125+7819	4.20	12.0	15.4	1.1	–	–	V	–	–	–	V
J1216−6410	3.54	47.4	4.0	1.2	–	–	–	–	–	V	–
J1300+1240[a]	6.22	10.2	25.3	0.4	–	–	–	–	–	–	V
J1312+0051	4.23	15.3	38.5	0.2	–	–	V	–	–	–	–
J1327−0755	2.68	27.9	8.4	0.2	–	–	–	–	–	V	–
J1327+3423	41.51	4.2	–	–	–	–	–	–	V	–	–
J1400−1431	3.08	4.9	9.5	0.2	–	–	–	–	–	–	V
J1421−4409	6.39	54.6	30.7	1.3	–	–	–	–	–	V	–
J1431−5740	4.11	131.4	2.7	0.4	–	–	–	–	–	V	–
J1435−6100	9.35	113.8	1.4	0.3	–	–	–	–	–	V	–
J1446−4701	2.20	55.8	0.3	0.5	–	–	–	V	–	V	–
J1453+1902	5.79	14.1	–	0.2	–	–	V	–	V	–	–
J1455−3330	7.99	13.6	76.2	0.7	V	–	V	–	–	V	–
J1525−5545	11.36	127.0	1.0	0.4	–	–	–	–	–	V	–
J1543−5149	2.06	51.0	8.1	0.8	–	–	–	–	–	V	–
J1544+4937	2.16	23.2	0.1	–	–	–	–	–	–	–	V
J1545−4550	3.58	68.4	6.2	1.1	–	–	–	V	–	V	–
J1547−5709	4.29	95.7	3.1	0.3	–	–	–	–	–	V	–
J1552+5437	2.43	22.9	–	–	–	–	–	–	–	–	V
J1600−3053	3.60	52.3	14.3	2.4	V	V	V	V	–	V	–
J1603−7202	14.84	38.0	6.3	2.5	–	–	–	V	–	V	–
J1614−2230	3.15	34.5	8.7	1.1	–	–	V	–	–	V	–
J1629−6902	6.00	29.5	–	1.0	–	–	–	–	–	V	–
J1630+3734	3.32	14.2	12.5	–	–	–	V	–	V	–	–
J1640+2224	3.16	18.4	175.5	0.5	V	–	V	–	V	–	V
J1643−1224	4.62	62.4	147.0	3.8	–	V	V	V	V	V	–
J1652−4838	3.79	188.2	–	0.9	–	–	–	–	–	V	–
J1653−2054	4.13	56.5	1.2	0.6	–	–	–	–	–	V	–

(*continued on next page*)

Table A.3 (*continued*).

Name	Period	DM	P_b	S_{1400}	Observed by						
(J2000)	(ms)	(pc/cm^3)	(days)	(mJy)	EPTA	InPTA	NANOGrav	PPTA	CPTA	MPTA	LOFAR
J1658+3630	33.03	3.0	3.0	–	–	–	–	–	–	–	V
J1658−5324	2.44	30.8	–	0.4	–	–	–	–	–	V	–
J1705−1903	2.48	57.5	–	0.6	–	–	V	–	–	V	–
J1708−3506	4.51	146.8	149.1	1.5	–	–	–	–	–	V	–
J1710+4923	3.22	7.1	–	–	–	–	–	–	V	–	–
J1713+0747	4.57	16.0	67.8	8.3	V	V	V	V	V	V	V
J1719−1438	5.79	36.8	0.1	0.4	–	–	V	–	–	V	–
J1721−2457	3.50	48.2	–	0.6	–	–	–	–	–	V	–
J1730−2304	8.12	9.6	–	4.0	V	–	V	V	–	V	V
J1732−5049	5.31	56.8	5.3	2.1	–	–	–	–	–	V	–
J1737−0811	4.18	55.3	79.5	1.1	–	–	–	–	–	V	–
J1738+0333	5.85	33.8	0.4	0.3	V	–	V	–	V	–	V
J1741+1351	3.75	24.2	16.3	0.3	–	–	V	V	V	–	–
J1744−1134	4.08	3.1	–	2.6	V	V	V	V	V	V	V
J1745+1017	2.65	24.0	0.7	0.5	–	–	V	–	V	–	–
J1747−4036	1.65	152.9	–	1.5	–	–	V	–	–	V	–
J1751−2857	3.92	42.8	110.7	0.5	V	–	V	–	–	V	–
J1756−2251	28.46	121.2	0.3	1.1	–	–	–	–	–	V	–
J1757−5322	8.87	30.8	0.5	1.2	–	–	–	–	–	V	–
J1801−1417	3.63	57.3	–	1.5	V	–	–	–	–	V	–
J1802−2124	12.65	149.6	0.7	0.7	–	–	V	–	–	V	–
J1804−2717	9.34	24.7	11.1	0.4	V	–	–	–	–	–	–
J1811−2405	2.66	60.6	6.3	1.3	–	–	V	–	–	V	–
J1824−2452	3.05	119.9	–	2.3	–	–	–	V	–	–	–
J1825−0319	4.55	119.6	52.6	0.2	–	–	–	–	–	V	–
J1832−0836	2.72	28.2	–	0.9	–	–	V	V	V	V	–
J1843−1113	1.85	60.0	–	0.1	V	–	V	–	V	V	–
J1853+1303	4.09	30.6	115.7	0.5	–	–	V	–	V	–	V
J1857+0943[b]	5.36	13.3	12.3	5.0	V	V	V	V	V	–	V
J1902−5105	1.74	36.3	2.0	1.0	–	–	–	V	–	V	–
J1903+0327	2.15	297.5	95.2	0.6	–	–	V	–	V	–	–
J1903−7051	3.60	19.7	11.1	1.0	–	–	–	–	–	V	–
J1909−3744	2.95	10.4	1.5	1.8	V	V	V	V	–	V	–
J1910+1256	4.98	38.1	58.5	0.7	V	–	V	–	V	–	–
J1911−1114	3.63	31.0	2.7	1.0	–	–	–	–	V	–	V
J1911+1347	4.63	31.0	–	0.9	V	–	V	–	V	–	–
J1918−0642	7.65	26.6	10.9	0.6	V	–	V	–	V	V	V
J1923+2515	3.79	18.9	–	0.2	–	–	V	–	V	–	V
J1933−6211	3.54	11.5	12.8	1.0	–	–	–	V	–	V	–
J1939+2134[c]	1.56	71.0	–	13.9	–	V	V	V	–	–	–
J1944+0907	5.19	24.4	–	2.1	–	–	V	–	V	–	V
J1946+3417	3.17	110.2	27.0	0.9	–	–	V	–	V	–	–
J1946−5403	2.71	23.7	0.1	0.4	–	–	–	–	–	V	–
J1955+2908[d]	6.13	104.5	117.3	1.0	–	–	V	–	V	–	V
J2010−1323	5.22	22.2	–	0.7	–	–	V	–	V	V	–
J2017+0603	2.90	23.9	2.2	0.2	–	–	V	–	V	–	–
J2019+2425	3.94	17.2	76.5	0.3	–	–	–	–	V	–	–
J2022+2534	2.65	53.7	–	–	–	–	–	–	V	–	–
J2033+1734	5.95	25.1	56.3	0.3	–	–	V	–	V	–	–
J2039−3616	3.28	24.0	5.8	0.5	–	–	–	–	–	V	–
J2043+1711	2.38	20.7	1.5	0.1	–	–	V	–	V	–	V
J2051−0827	4.51	20.7	0.1	2.8	–	–	–	–	–	–	V
J2124−3358	4.93	4.6	–	4.5	V	V	V	V	–	V	–
J2129−5721	3.73	31.8	6.6	1.0	–	–	–	V	–	V	–
J2145−0750	16.05	9.0	6.8	5.5	–	V	V	V	V	V	V
J2150−0326	3.50	20.7	–	0.5	–	–	–	–	V	V	–
J2214+3000	3.12	22.5	0.4	0.5	–	–	V	–	V	–	–
J2222−0137	32.82	3.3	2.4	0.9	–	–	–	–	–	V	V
J2229+2643	2.98	22.7	93.0	0.8	–	–	V	–	V	V	–
J2234+0611	3.58	10.8	32.0	0.5	–	–	V	–	V	–	–
J2234+0944	3.63	17.8	0.4	1.9	–	–	V	–	V	V	–
J2241−5236	2.19	11.4	0.1	1.8	–	–	–	V	–	V	–
J2302+4442	5.19	13.8	125.9	1.4	–	–	V	–	V	–	V
J2317+1439	3.45	21.9	2.5	0.6	–	–	V	–	V	V	V
J2322+2057	4.81	13.4	–	0.3	V	–	V	–	V	V	–
J2322−2650	3.46	6.1	0.3	0.2	–	–	–	–	–	V	–

[a] PSR J1300+1240 is also referred to as PSR B1257+12.

[b] PSR J1857+0943 is also referred to as PSR B1855+09.

[c] PSR J1939+2134 is also referred to as PSR B1937+21.

[d] PSR J1955+2908 is also referred to as PSR B1953+29.

Table B.4
Characteristics of PTA observations. For each PTA the different participating observatories are given, along with the current observing frequencies and maximal bandwidths in the different observing bands. The time span corresponds to the range of dates over which PTA observations were carried out at the observatories, including with older systems that are not detailed in this table. Unless otherwise specified, the first reference given for a PTA refers to all telescopes of that PTA. The first four PTAs in this list (EPTA, InPTA, NANOGrav and PPTA) are all members of the IPTA, which also has a data-sharing agreement with the MPTA.

PTA	Telescope	f_c (MHz)	BW (MHz)	Timespan	Ref.
EPTA	Effelsberg (EFF)	1380, 2487, 4857	240, 300, 500	1996–	Antoniadis et al. [43]
	Lovell[a] (JBO)	1532	512	2009–	
	Nançay (NRT)	1484, 1854, 2154, 2539	512	2004–	
	Sardinia (SRT)	357, 1396	105, 500	2014–	
	Westerbork (WSRT)	350, 1380, 2273	80, 160, 160	1999–2015	
	LEAP	1396	128	2012–	Bassa et al. [42]
	LOFAR	148.9	78.1	2012–	Donner et al. [46]
InPTA	GMRT	400, 1360	200	2018–	Tarafdar et al. [50]
NANOGrav[b]	Arecibo (AO)	327, 433, 1456, 2052	50, 24, 600, 460	2004–2020	Agazie et al. [51]
	Green Bank (GBT)	820, 1518	180, 640	2004–	
	VLA	1520, 3000	800, 1700	2015–	
	CHIME	600	400	2019–	Amiri et al. [52]
PPTA	Parkes (PKS)	2368[c]	3328	2004–	Zic et al. [54]
MPTA	MeerKAT	1284	856	2019–	Miles et al. [37]
CPTA	FAST	1250	500	2019–	Xu et al. [56]

[a] For PSR J1713+0747, the Jodrell Bank Observatory also provided data from the Mark II telescope. The observation's characteristics are identical to those listed above.
[b] For NANOGrav, the quoted bandwidths are the *usable* bandwidth, accounting for RFI excision.
[c] The PPTA presently uses an ultra-wide-bandwidth receiver with continuous frequency coverage from 704 to 4032 MHz. In practice they split up this bandpass in eight sub-bands with center frequencies ranging from 736 to 3312 MHz.

Appendix A. List of PTA Pulsars

See Table A.3.

Appendix b. list of PTA telescopes and observing properties

See Table B.4.

References

[1] Lorimer DR. Binary and millisecond pulsars. Living Rev Relativ 2008;11:8–+, arXiv:0811.0762.
[2] Melrose DB, Rafat MZ, Mastrano A. Pulsar radio emission mechanisms: A critique. Mon Not R Astron Soc 2021;500:4530–48. http://dx.doi.org/10.1093/mnras/staa3324, arXiv:2006.15243.
[3] Hewish A, Bell SJ, Pilkington JDH, Scott PF, Collins RA. Observation of a rapidly pulsating radio source. Nature 1968;217:709–13.
[4] Verbiest JPW, Shaifullah G. Measurement uncertainty in pulsar timing array experiments. Classical Quantum Gravity 2018;35.
[5] Lorimer DR, Kramer M. Handbook of pulsar astronomy. Cambridge University Press; 2005.
[6] Sazhin MV. Opportunities for detecting ultralong gravitational waves. Sov Astron 1978;22(36).
[7] Detweiler S. Pulsar timing measurements and the search for gravitational waves. Astrophys J 1979;234:1100.
[8] Hellings RW, Downs GS. Upper limits on the isotropic gravitational radiation background from pulsar timing analysis. Astrophys J 1983;265.
[9] Foster RS, Backer DC. Constructing a pulsar timing array. Astrophys J 1990;361:300.
[10] Romani RW. Timing a millisecond pulsar array. In: Ögelman H, van den Heuvel EPJ, editors. Timing neutron stars. 1989, p. 113–7.
[11] Hobbs G, Guo L, Caballero RN, Coles W, Lee KJ, Manchester RN, et al. A pulsar-based time-scale from the international pulsar timing array. Mon Not R Astron Soc 2020;491:5951–65. http://dx.doi.org/10.1093/mnras/stz3071, arXiv:1910.13628.
[12] Caballero RN, Guo YJ, Lee KJ, Lazarus P, Champion DJ, Desvignes G, et al. Studying the solar system with the international pulsar timing array. Mon Not R Astron Soc 2018;481:5501–16. http://dx.doi.org/10.1093/mnras/sty2632, arXiv:1809.10744.
[13] Guo YJ, Li GY, Lee KJ, Caballero RN. Studying the solar system dynamics using pulsar timing arrays and the LINIMOSS dynamical model. Mon Not R Astron Soc 2019;489:5573–81. http://dx.doi.org/10.1093/mnras/stz2515, arXiv:1909.04507.
[14] Vallisneri M, Taylor SR, Simon J, Folkner WM, Park RS, Cutler C, et al. Modeling the uncertainties of solar system ephemerides for robust gravitational-wave searches with pulsar-timing arrays. Astrophys J 2020;893:112. http://dx.doi.org/10.3847/1538-4357/ab7b67, arXiv:2001.00595.
[15] Taylor SR. Nanohertz gravitational wave astronomy. CRC Press; 2021.
[16] Verbiest JPW, Osłowski S, Burke-Spolaor S. Pulsar timing array experiments. In: Handbook of gravitational wave astronomy. 2021, p. 4. http://dx.doi.org/10.1007/978-981-15-4702-7_4-1.
[17] Lommen AN. Pulsar timing arrays: The promise of gravitational wave detection. Rep Progr Phys 2015;78:124901. http://dx.doi.org/10.1088/0034-4885/78/12/124901.
[18] Hobbs G, Dai S. Gravitational wave research using pulsar timing arrays. Natl. Sci. Revi. 2017;4:707–17. http://dx.doi.org/10.1093/nsr/nwx126, arXiv:https://academic.oup.com/nsr/article-pdf/4/5/707/31566772/nwx126.pdf.
[19] Tiburzi C. Pulsars probe the low-frequency gravitational sky: Pulsar timing arrays basics and recent results. PASA 2018;35:e013. http://dx.doi.org/10.1017/pasa.2018.7, arXiv:1802.05076.
[20] Burke-Spolaor S, Taylor SR, Charisi M, Dolch T, Hazboun JS, Holgado AM, et al. The astrophysics of nanohertz gravitational waves. Astron. Astropys. Rev. 2019;27:5. http://dx.doi.org/10.1007/s00159-019-0115-7, arXiv:1811.08826.
[21] Perrodin D, Sesana A. In: Rezzolla L, Pizzochero P, Jones DI, Rea N, Vidaña I, editors. Radio pulsars: Testing gravity and detecting gravitational waves. Astrophysics and Space Science Library; 2018, p. 95. http://dx.doi.org/10.1007/978-3-319-97616-7_3, arXiv:1709.02816.
[22] Bak Nielsen AS, Janssen GH, Shaifullah G, Verbiest JPW, Champion DJ, Desvignes G, et al. Timing stability of three black widow pulsars. Mon Not R Astron Soc 2020;494:2591–9. http://dx.doi.org/10.1093/mnras/staa874, arXiv:2003.10352.
[23] Desvignes G, Caballero RN, Lentati L, Verbiest JPW, Champion DJ, Stappers BW, et al. High-precision timing of 42 millisecond pulsars with the European pulsar timing array. Mon Not R Astron Soc 2016;458:3341–80. http://dx.doi.org/10.1093/mnras/stw483, arXiv:1602.08511.
[24] Johnston S, Lorimer DR, Harrison PA, Bailes M, Lyne AG, Bell JF, et al. Discovery of a very bright, nearby binary millisecond pulsar. Nature 1993;361:613–5.
[25] Manchester RN, Lyne AG, Camilo F, Bell JF, Kaspi VM, D'Amico N, et al. The Parkes multi-beam pulsar survey - I. Observing and data analysis systems, discovery and timing of 100 pulsars. Mon Not R Astron Soc 2001;328:17–35.
[26] Edwards RT, Bailes M. Discovery of two relativistic neutron star – white dwarf binaries. Astrophys J 2001;547:L37–40.
[27] Verbiest JPW, Bailes M, Coles WA, Hobbs GB, van Straten W, Champion DJ, et al. Timing stability of millisecond pulsars and prospects for gravitational-wave detection. Mon Not R Astron Soc 2009;400:951–68, arXiv:0908.0244.
[28] Lorimer DR, Faulkner AJ, Lyne AG, Manchester RN, Kramer M, McLaughlin MA, et al. The Parkes multibeam pulsar survey - VI. Discovery and timing of 142 pulsars and a galactic population analysis. Mon Not R Astron Soc 2006;372:777–800.
[29] Manchester RN, Hobbs G, Bailes M, Coles WA, van Straten W, Keith MJ, et al. The Parkes pulsar timing array project. PASA 2013;30:17. http://dx.doi.org/10.1017/pasa.2012.017, arXiv:1210.6130.
[30] Demorest PB, Ferdman RD, Gonzalez ME, Nice D, Ransom S, Stairs IH, et al. Limits on the stochastic gravitational wave background from the North American nanohertz observatory for gravitational waves. Astrophys J 2013;762:94. http://dx.doi.org/10.1088/0004-637X/762/2/94, arXiv:1201.6641.

[31] Manchester RN, IPTA. The international pulsar timing array. Classical Quantum Gravity 2013;30:224010. http://dx.doi.org/10.1088/0264-9381/30/22/224010, arXiv:1309.7392.

[32] Verbiest JPW, Lentati L, Hobbs G, van Haasteren R, Demorest PB, Janssen GH, et al. The international pulsar timing array: First data release. Mon Not R Astron Soc 2016;458:1267–88. http://dx.doi.org/10.1093/mnras/stw347, arXiv:1602.03640.

[33] Perera BBP, DeCesar ME, Demorest PB, Kerr M, Lentati L, Nice DJ, et al. The international pulsar timing array: Second data release. Mon Not R Astron Soc 2019;490:4666–87. http://dx.doi.org/10.1093/mnras/stz2857, arXiv:1909.04534.

[34] Joshi BC, Arumugasamy P, Bagchi M, Bandyopadhyay D, Basu A, Dhanda Batra N, et al. Precision pulsar timing with the ORT and the GMRT and its applications in pulsar astrophysics. J Astrophys Astron 2018;39:51. http://dx.doi.org/10.1007/s12036-018-9549-y.

[35] Joshi BC, Gopakumar A, Pandian A, Prabu T, Dey L, Bagchi M, et al. Nanohertz gravitational wave astronomy during SKA era: An InPTA perspective. J Astrophys Astron 2022;43:98. http://dx.doi.org/10.1007/s12036-022-09869-w, arXiv:2207.06461.

[36] Lee KJ. Prospects of gravitational wave detection using pulsar timing array for Chinese future telescopes. In: Qain L, Li D, editors. Frontiers in radio astronomy and FAST early sciences symposium 2015. 2016, p. 19.

[37] Miles MT, Shannon RM, Bailes M, Reardon DJ, Keith MJ, Cameron AD, et al. The MeerKAT pulsar timing array: first data release. Mon Not R Astron Soc 2023;519:3976–91. http://dx.doi.org/10.1093/mnras/stac3644, arXiv:2212.04648.

[38] Rodin AE. Detection of gravitational waves through observations of a group of pulsars. Astron Rep 2011;55:132–41. http://dx.doi.org/10.1134/S1063772911020053, arXiv:1101.0063.

[39] Gancio G, Lousto CO, Combi L, Palacio Sdel, López Armengol FG, Combi JA, et al. Upgraded antennas for pulsar observations in the Argentine Institute of Radio astronomy. Astron Astrophys 2020;633:A84. http://dx.doi.org/10.1051/0004-6361/201936525, arXiv:1908.07049.

[40] Sosa Fiscella V, del Palacio S, Combi L, Lousto CO, Combi JA, Gancio G, et al. PSR J0437-4715: The Argentine Institute of Radioastronomy 2019–2020 observational campaign. Astrophys J 2021;908:158. http://dx.doi.org/10.3847/1538-4357/abceb3, arXiv:2010.00010.

[41] FERMI-LAT Collaboration Ajello M, Atwood WB, Baldini L, Ballet J, Barbiellini G, Bastieri D, et al. A gamma-ray pulsar timing array constrains the nanohertz gravitational wave background. Science 2022;376:521–3. http://dx.doi.org/10.1126/science.abm3231, arXiv:2204.05226.

[42] Bassa CG, Janssen GH, Karuppusamy R, Kramer M, Lee KJ, Liu K, et al. LEAP: The large European array for pulsars. Mon Not R Astron Soc 2016;456:2196–209. http://dx.doi.org/10.1093/mnras/stv2755, arXiv:1511.06597.

[43] EPTA Collaboration Antoniadis J, Babak S, Bak Nielsen AS, Bassa CG, Berthereau A, Bonetti M, et al. The second data release from the European pulsar timing array. I. The dataset and timing analysis. Astron Astrophys 2023;678:A48. http://dx.doi.org/10.1051/0004-6361/202346841, arXiv:2306.16224.

[44] van Haarlem MP, Wise MW, Gunst AW, Heald G, McKean JP, Hessels JWT, et al. LOFAR: The LOw-frequency array. Astron Astrophys 2013;556:A2. http://dx.doi.org/10.1051/0004-6361/201220873, arXiv:1305.3550.

[45] Kondratiev VI, Verbiest JPW, Hessels JWT, Bilous AV, Stappers BW, Kramer M, et al. A LOFAR census of millisecond pulsars. Astron Astrophys 2016;585:A128. http://dx.doi.org/10.1051/0004-6361/201527178, arXiv:1508.02948.

[46] Donner JY, Verbiest JPW, Tiburzi C, Osłowski S, Künsemöller J, Bak Nielsen AS, et al. Dispersion measure variability for 36 millisecond pulsars at 150 MHz with LOFAR. Astron Astrophys 2020;644. http://dx.doi.org/10.1051/0004-6361/202039517, arXiv:2011.13742.

[47] Bondonneau L, Grießmeier JM, Theureau G, Cognard I, Brionne M, Kondratiev V, et al. Pulsars with NenuFAR: Backend and pipelines. Astron Astrophys 2021;652:A34. http://dx.doi.org/10.1051/0004-6361/202039339, arXiv:2009.02076.

[48] Speri L, Porayko NK, Falxa M, Chen S, Gair JR, Sesana A, et al. Quality over quantity: Optimizing pulsar timing array analysis for stochastic and continuous gravitational wave signals. Mon Not R Astron Soc 2023;518:1802–17. http://dx.doi.org/10.1093/mnras/stac3237, arXiv:2211.03201.

[49] Lazarus P, Karuppusamy R, Graikou E, Caballero RN, Champion DJ, Lee KJ, Verbiest JPW, Kramer M. Prospects for high-precision pulsar timing with the new Effelsberg PSRIX backend. Mon Not R Astron Soc 2016;458:868–80. http://dx.doi.org/10.1093/mnras/stw189, arXiv:1601.06194.

[50] Tarafdar P, Nobleson K, Rana P, Singha J, Krishnakumar MA, Joshi BC, et al. The Indian pulsar timing array: First data release. PASA 2022;39:e053. http://dx.doi.org/10.1017/pasa.2022.46, arXiv:2206.09289.

[51] Agazie G, Alam MF, Anumarlapudi A, Archibald AM, Arzoumanian Z, Baker PT, et al., Nanograv Collaboration. The NANOGrav 15 yr data set: Observations and timing of 68 millisecond pulsars. Astrophys J 2023;951:L9. http://dx.doi.org/10.3847/2041-8213/acda9a, arXiv:2306.16217.

[52] CHIME/Pulsar Coll. Amiri M, Bandura KM, Boyle PJ, Brar C, Cliche JF, et al. The CHIME pulsar project: System overview. Astrophys J Suppl 2021;255:5. http://dx.doi.org/10.3847/1538-4365/abfdcb, arXiv:2008.05681.

[53] Good DC. Timing pulsars and detecting radio transients with cHIME. [Ph.D. thesis], University of British Columbia; 2021.

[54] Zic A, Reardon DJ, Kapur A, Hobbs G, Mandow R, Curyło M, et al. The Parkes pulsar timing array third data release. PASA 2023;40:e049. http://dx.doi.org/10.1017/pasa.2023.36, arXiv:2306.16230.

[55] Hobbs G, Manchester RN, Dunning A, Jameson A, Roberts P, George D, et al. An ultra-wide bandwidth (704 to 4 032 MHz) receiver for the Parkes radio telescope. PASA 2020;37:e012. http://dx.doi.org/10.1017/pasa.2020.2, arXiv:1911.00656.

[56] Xu H, Chen S, Guo Y, Jiang J, Wang B, Xu J, et al. Searching for the nanohertz stochastic gravitational wave background with the Chinese pulsar timing array data release I. Res Astron Astrophys 2023;23:075024. http://dx.doi.org/10.1088/1674-4527/acdfa5, arXiv:2306.16216.

[57] van Straten W, Bailes M. DSPSR: Digital signal processing software for pulsar astronomy. PASA 2011;28:1–14. http://dx.doi.org/10.1071/AS10021, arXiv:1008.3973.

[58] DuPlain R, Ransom S, Demorest P, Brandt P, Ford J, Shelton AL. Launching GUPPI: the green bank ultimate pulsar processing instrument. In: Bridger A, Radziwill NM, editors. Advanced software and control for astronomy II. 2008, p. 70191D. http://dx.doi.org/10.1117/12.790003.

[59] Hotan AW, Straten Wvan, Manchester RN. PSRCHIVE and PSRFITS: An open approach to radio pulsar data storage and analysis. PASA 2004;21:302–9.

[60] van Straten W, Demorest P, Oslowski S. Pulsar data analysis with PSRCHIVE. Astron Res Technol 2012;9:237–56, arXiv:1205.6276.

[61] Wang J, Shaifullah GM, Verbiest JPW, Tiburzi C, Champion DJ, Cognard I, et al. A comparative analysis of pulse time-of-arrival creation methods. Astron Astrophys 2022;658:A181. http://dx.doi.org/10.1051/0004-6361/202141121, arXiv:2111.13482.

[62] Hobbs GB, Edwards RT, Manchester RN. Tempo2, a new pulsar-timing package - I. An overview. Mon Not R Astron Soc 2006;369:655–72. http://dx.doi.org/10.1111/j.1365-2966.2006.10302.x, arXiv:astro-ph/0603381.

[63] Luo J, Ransom S, Demorest P, Ray PS, Archibald A, Kerr M, et al. PINT: A modern software package for pulsar timing. Astrophys J 2021;911:45. http://dx.doi.org/10.3847/1538-4357/abe62f, arXiv:2012.00074.

[64] Edwards RT, Hobbs GB, Manchester RN. TEMPO2, a new pulsar timing package - II. The timing model and precision estimates. Mon Not R Astron Soc 2006;372:1549–74. http://dx.doi.org/10.1111/j.1365-2966.2006.10870.x, arXiv:astro-ph/0607664.

[65] Ellis JA, Vallisneri M, Taylor SR, Baker PT. ENTERPRISE: Enhanced numerical toolbox enabling a robust pulsar inference SuitE. 2019, Astrophysics Source Code Library, record ascl:1912.015. arXiv:1912.015.

[66] Lentati L, Alexander P, Hobson MP, Feroz F, van Haasteren R, Lee KJ, et al. TEMPONEST: A Bayesian approach to pulsar timing analysis. Mon Not R Astron Soc 2014;437:3004–23. http://dx.doi.org/10.1093/mnras/stt2122, arXiv:1310.2120.

[67] Anholm M, Ballmer S, Creighton JDE, Price LR, Siemens X. Optimal strategies for gravitational wave stochastic background searches in pulsar timing data. Phys Rev D 2009;79:084030. http://dx.doi.org/10.1103/PhysRevD.79.084030, arXiv:0809.0701.

[68] Chamberlin SJ, Creighton JDE, Siemens X, Demorest P, Ellis J, Price LR, et al. Time-domain implementation of the optimal cross-correlation statistic for stochastic gravitational-wave background searches in pulsar timing data. Phys Rev D 2015;91:044048. http://dx.doi.org/10.1103/PhysRevD.91.044048, arXiv:1410.8256.

[69] Vigeland SJ, Islo K, Taylor SR, Ellis JA. Noise-marginalized optimal statistic: A robust hybrid frequentist-Bayesian statistic for the stochastic gravitational-wave background in pulsar timing arrays. Phys Rev D 2018;98:044003. http://dx.doi.org/10.1103/PhysRevD.98.044003, arXiv:1805.12188.

[70] Ellis JA, Siemens X, Creighton JDE. Optimal strategies for continuous gravitational wave detection in pulsar timing arrays. Astrophys J 2012;756:175. http://dx.doi.org/10.1088/0004-637X/756/2/175, arXiv:1204.4218.

[71] Lamb WG, Taylor SR, van Haasteren R. Rapid refitting techniques for Bayesian spectral characterization of the gravitational wave background using pulsar timing arrays. Phys Rev D 2023;108:103019. http://dx.doi.org/10.1103/PhysRevD.108.103019, arXiv:2303.15442.

[72] Shannon RM, Cordes JM. Assessing the role of spin noise in the precision timing of millisecond pulsars. Astrophys J 2010;725:1607–19. http://dx.doi.org/10.1088/0004-637X/725/2/1607, arXiv:1010.4794.

[73] Verbiest JPW, Bailes M, van Straten W, Hobbs GB, Edwards RT, Manchester RN, et al. Precision timing of psr j0437–4715: An accurate pulsar distance, a high pulsar mass, and a limit on the variation of Newton's gravitational constant. Astrophys J 2008;679:675–80, arXiv:arXiv:0801.2589.

[74] Coles W, Hobbs G, Champion DJ, Manchester RN, Verbiest JPW. Pulsar timing analysis in the presence of correlated noise. Mon Not R Astron Soc 2011;418:561–70. http://dx.doi.org/10.1111/j.1365-2966.2011.19505.x, arXiv:1107.5366.

[75] Hobbs G, Lyne AG, Kramer M. An analysis of the timing irregularities for 366 pulsars. Mon Not R Astron Soc 2010;402:1027–48. http://dx.doi.org/10.1111/j.1365-2966.2009.15938.x, arXiv:0912.4537.

[76] Agazie G, Anumarlapudi A, Archibald AM, Arzoumanian Z, Baker PT, Bécsy B, et al., Nanograv Collaboration. The NANOGrav 15 yr data set: Detector characterization and noise budget. Astrophys J 2023;951:L10. http://dx.doi.org/10.3847/2041-8213/acda88, arXiv:2306.16218.

[77] EPTA Collaboration and InPTA Collaboration Antoniadis J, Arumugam P, Arumugam S, Babak S, Bagchi M, Nielsen ASB, et al. The second data release from the European pulsar timing array. II. Customised pulsar noise models for spatially correlated gravitational waves. Astron Astrophys 2023;678:A49. http://dx.doi.org/10.1051/0004-6361/202346842, arXiv:2306.16225.

[78] Srivastava A, Desai S, Kolhe N, Surnis M, Joshi BC, Susobhanan A, et al. Noise analysis of the Indian pulsar timing array data release I. Phys Rev D 2023;108:023008. http://dx.doi.org/10.1103/PhysRevD.108.023008, arXiv:2303.12105.

[79] Goncharov B, Reardon DJ, Shannon RM, Zhu XJ, Thrane E, Bailes M, et al. Identifying and mitigating noise sources in precision pulsar timing data sets. Mon Not R Astron Soc 2021;502:478–93. http://dx.doi.org/10.1093/mnras/staa3411, arXiv:2010.06109.

[80] Reardon DJ, Zic A, Shannon RM, Di Marco V, Hobbs GB, Kapur A, et al. The gravitational-wave background null hypothesis: Characterizing noise in millisecond pulsar arrival times with the Parkes pulsar timing array. Astrophys J 2023;951:L7. http://dx.doi.org/10.3847/2041-8213/acdd03, arXiv:2306.16229.

[81] Janssen G, Hobbs G, McLaughlin M, Bassa C, Deller A, Kramer M, et al. Gravitational wave astronomy with the SKA. Advanc Astrophys Square Kilometre Array (AASKA14) 2015;37. arXiv:1501.00127.

[82] Lam MT, Ellis JA, Grillo G, Jones ML, Hazboun JS, Brook PR, et al. A second chromatic timing event of interstellar origin toward PSR J1713+0747. Astrophys J 2018;861:132. http://dx.doi.org/10.3847/1538-4357/aac770, arXiv:1712.03651.

[83] Pennucci TT, Demorest PB, Ransom SM. Elementary wideband timing of radio pulsars. Astrophys J 2014;790:93. http://dx.doi.org/10.1088/0004-637X/790/2/93, arXiv:1402.1672.

[84] Paladi AK, Dwivedi C, Rana P, Nobleson K, Susobhanan A, Joshi BC, et al. Multiband extension of the wideband timing technique. Mon Not R Astron Soc 2024;527:213–31. http://dx.doi.org/10.1093/mnras/stad3122, arXiv:2304.13072.

[85] Curyło M, Pennucci TT, Bailes M, Bhat NDR, Cameron AD, Dai S, et al. Wide-band timing of the parkes pulsar timing array UWL data. Astrophys J 2023;944:128. http://dx.doi.org/10.3847/1538-4357/aca535, arXiv:2211.12924.

[86] Lentati L, Kerr M, Dai S, Hobson MP, Shannon RM, Hobbs G, et al. Wide-band profile domain pulsar timing analysis. Mon Not R Astron Soc 2017;466:3706–27. http://dx.doi.org/10.1093/mnras/stw3359, arXiv:1612.05258.

[87] Cordes JM, Shannon RM, Stinebring DR. Frequency-dependent dispersion measures and implications for pulsar timing. Astrophys J 2016;817:16. http://dx.doi.org/10.3847/0004-637X/817/1/16, arXiv:1503.08491.

[88] Donner JY, Verbiest JPW, Tiburzi C, Osłowski S, Michilli D, Serylak M, et al. First detection of frequency-dependent, time-variable dispersion measures. Astron Astrophys 2019;624:A22. http://dx.doi.org/10.1051/0004-6361/201834059, arXiv:1902.03814.

[89] Lentati L, Shannon RM, Coles WA, Verbiest JPW, van Haasteren R, Ellis JA, et al. From spin noise to systematics: stochastic processes in the first international pulsar timing array data release. Mon Not R Astron Soc 2016;458:2161–87. http://dx.doi.org/10.1093/mnras/stw395, arXiv:1602.05570.

[90] Shannon RM, Lentati LT, Kerr M, Bailes M, Bhat NDR, Coles WA, et al. The disturbance of a millisecond pulsar magnetosphere. Astrophys J 2016;828:L1. http://dx.doi.org/10.3847/2041-8205/828/1/L1, arXiv:1608.02163.

[91] Krishnakumar MA, Manoharan PK, Joshi BC, Girgaonkar R, Desai S, Bagchi M, et al. High precision measurements of interstellar dispersion measure with the upgraded GMRT. Astron Astrophys 2021;651:A5. http://dx.doi.org/10.1051/0004-6361/202140340, arXiv:2101.05334.

[92] Caballero RN, Lee KJ, Lentati L, Desvignes G, Champion DJ, Verbiest JPW, et al. The noise properties of 42 millisecond pulsars from the European pulsar timing array and their impact on gravitational-wave searches. Mon Not R Astron Soc 2016;457:4421–40. http://dx.doi.org/10.1093/mnras/stw179, arXiv:1510.09194.

[93] Fumagalli G, Shaifullah G, Sesana A. The impact of outliers on pulsar timing arrays. 2023, http://dx.doi.org/10.48550/arXiv.2311.01505, arXiv e-prints, MNRAS Accepted, arXiv:2311.01505.

[94] International Pulsar Timing Array Collaboration Agazie G, Antoniadis J, Anumarlapudi A, Archibald AM, Arumugam P, Arumugam S, et al. Comparing recent PTA results on the nanohertz stochastic gravitational wave background. 2023, http://dx.doi.org/10.48550/arXiv.2309.00693, arXiv e-prints, ApJ Accepted, arXiv:2309.00693.

[95] Lin FX, Lin HH, Luo J, Main R, McKee J, Pen UL, et al. Profile changes associated with dispersion measure events in PSR J1713+0747. Mon Not R Astron Soc 2021;508:1115–27. http://dx.doi.org/10.1093/mnras/stab2529, arXiv:2106.09851.

[96] Singha J, Surnis MP, Joshi BC, Tarafdar P, Rana P, Susobhanan A, et al. Evidence for profile changes in PSR J1713+0747 using the uGMRT. Mon Not R Astron Soc 2021;507:L57–61. http://dx.doi.org/10.1093/mnrasl/slab098, arXiv:2107.04607.

[97] Lam MT. Evidence for multiple pulse-shape changes during the third chromatic timing event of PSR J1713 + 0747. Res Not Am Astron Soc 2021;5:167. http://dx.doi.org/10.3847/2515-5172/ac1670.

[98] Jennings RJ, Cordes JM, Chatterjee S, McLaughlin MA, Demorest PB, Arzoumanian Z, et al. An unusual pulse shape change event in PSR J1713+0747 observed with the green bank telescope and CHIME. 2022, http://dx.doi.org/10.48550/arXiv.2210.12266, arXiv e-prints, arXiv:2210.12266.

[99] Arzoumanian Z, Baker PT, Blumer H, Bécsy B, Brazier A, Brook PR, et al., Nanograv Collaboration. The NANOGrav 12.5 yr data set: Search for an isotropic stochastic gravitational-wave background. Astrophys J 2020;905:L34. http://dx.doi.org/10.3847/2041-8213/abd401, arXiv:2009.04496.

[100] Manoharan PK. Three-dimensional evolution of solar wind during solar cycles 22-24. Astrophys J 2012;751:128. http://dx.doi.org/10.1088/0004-637X/751/2/128, arXiv:1203.6715.

[101] You XP, Hobbs GB, Coles WA, Manchester RN, Han JL. An improved solar wind electron density model for pulsar timing. Astrophys J 2007;671:907–11, arXiv:0709.0135.

[102] Madison DR, Cordes JM, Arzoumanian Z, Chatterjee S, Crowter K, DeCesar ME, et al. The NANOGrav 11 yr data set: Solar wind sounding through pulsar timing. Astrophys J 2019;872:150. http://dx.doi.org/10.3847/1538-4357/ab01fd, arXiv:1808.07078.

[103] Tiburzi C, Shaifullah GM, Bassa CG, Zucca P, Verbiest JPW, Porayko NK, et al. The impact of solar wind variability on pulsar timing. Astron Astrophys 2021;647:A84. http://dx.doi.org/10.1051/0004-6361/202039846, arXiv:2012.11726.

[104] Tiburzi C, Verbiest JPW, Shaifullah GM, Janssen GH, Anderson JM, Horneffer A, et al. On the usefulness of existing solar wind models for pulsar timing corrections. Mon Not R Astron Soc 2019;487:394–408. http://dx.doi.org/10.1093/mnras/stz1278, arXiv:1905.02989.

[105] Susarla SC, Chalumeau A, Tiburzi C, Keane EF, Verbiest JPW, Hazboun JS, Krishnakumar MA, Iraci F, Shaifullah GM, Golden A, Grieß meier J-M, Bak Nielsen A-S, Ciardi B, Vocks C, Schwarz D, Künsemöller J, Donner J, Serylak M, Brüggen M, Keith MJ, Porayko NK, Dettmar R-J, Osłowski S. Exploring the time variability of the solar wind using LOFAR pulsar data. Astron Astrophys 2024. [submitted to A&A, May 2024].

[106] Nițu IC, Keith MJ, Tiburzi C, Brüggen M, Champion DJ, Chen S, et al. A Gaussian-processes approach to fitting for time-variable spherical solar wind in pulsar timing data. Mon Not R Astron Soc 2024;528:3304–19. http://dx.doi.org/10.1093/mnras/stae220, arXiv:2401.07917.

[107] Bisi MM, Fallows RA, Matyjasiak B, Rothkaehl H, Vermeulen R, Baldovin C, et al. LOFAR4SpaceWeather (LOFAR4SW) –increasing European space-weather capability with Europe's largest radio telescope: Summary and beyond the first major project. In: AGU fall meeting abstracts. 2022, pp. SH46B–03.

[108] Tiburzi C, Jackson BV, Cota L, Shaifullah GM, Fallows RA, Tokumaru M, Zucca P. Validation of heliospheric modeling algorithms through pulsar observations I: Interplanetary scintillation-based tomography. J Adv Space Res 2023. http://dx.doi.org/10.48550/arXiv.2306.07451, arXiv e-prints, arXiv:2306.07451.

[109] Shaifullah G, Tiburzi C, Zucca P. CMEchaser, detecting line-of-sight occultations due to coronal mass ejections. Sol Phys 2020;295:136. http://dx.doi.org/10.1007/s11207-020-01705-0, arXiv:2008.12153.

[110] Ord SM, Bailes M, van Straten W. The scintillation velocity of the relativistic binary pulsar PSR J1141-6545. Astrophys J 2002;574:L75–8.

[111] Reardon DJ, Coles WA, Hobbs G, Ord S, Kerr M, Bailes M, et al. Modelling annual and orbital variations in the scintillation of the relativistic binary PSR J1141-6545. Mon Not R Astron Soc 2019;485:4389–403. http://dx.doi.org/10.1093/mnras/stz643, arXiv:1903.01990.

[112] Reardon DJ, Coles WA, Bailes M, Bhat NDR, Dai S, Hobbs GB, et al. Precision orbital dynamics from interstellar scintillation arcs for PSR J0437-4715. Astrophys J 2020;904:104. http://dx.doi.org/10.3847/1538-4357/abbd40, arXiv:2009.12757.

[113] Fonseca E, Pennucci TT, Ellis JA, Stairs IH, Nice DJ, Ransom SM, et al. The NANOGrav nine-year data set: Mass and geometric measurements of binary millisecond pulsars. 2016, ArXiv e-prints arXiv:1603.00545.

[114] Walker K, Reardon DJ, Thrane E, Smith R. Orbital dynamics and extreme scattering event properties from long-term scintillation observations of PSR J1603-7202. Astrophys J 2022;933:16. http://dx.doi.org/10.3847/1538-4357/ac69c6, arXiv:2204.11077.

[115] Askew J, Reardon DJ, Shannon RM. Analysis of the ionized interstellar medium and orbital dynamics of PSR J1909-3744 using scintillation arcs. Mon Not R Astron Soc 2023;519:5086–98. http://dx.doi.org/10.1093/mnras/stac3095, arXiv:2210.13703.

[116] Liu Y, Main RA, Verbiest JPW, Wu Z, Ambalappat KM, Lu J, et al. Periodic interstellar scintillation variations of PSRs J0613-0200 and J0636+5128 associated with the local bubble shell. Sci China Phys, Mech Astron 2023;66:119512. http://dx.doi.org/10.1007/s11433-023-2182-6, arXiv:2307.09745.

[117] Main RA, Antoniadis J, Chen S, Cognard I, Hu H, Jang J, et al. Variable scintillation arcs of millisecond pulsars observed with the large European array for pulsars. Mon Not R Astron Soc 2023;525:1079–96. http://dx.doi.org/10.1093/mnras/stad1980, arXiv:2306.13462.

[118] Reardon DJ, Coles WA. Determining electron column density fluctuations in a dominant scattering region using pulsar scintillation. Mon Not R Astron Soc 2023;521:6392–400. http://dx.doi.org/10.1093/mnras/stad962, arXiv:2303.16338.

[119] Cordes JM, Rickett BJ. Diffractive interstellar scintillation timescales and velocities. Astrophys J 1998;507:846–60.

[120] Bhat NDR, Cordes JM, Camilo F, Nice DJ, Lorimer DR. Multifrequency observations of radio pulse broadening and constraints on interstellar electron density microstructure. Astrophys J 2004;605:759–83.

[121] Liu Y, Verbiest JPW, Main RA, Wu Z, Ambalappat KM, Champion DJ, et al. Long-term scintillation studies of EPTA pulsars. I. Observations and basic results. Astron Astrophys 2022;664:A116. http://dx.doi.org/10.1051/0004-6361/202142552, arXiv:2203.16950.

[122] Bansal K, Taylor GB, Stovall K, Dowell J. Scattering study of pulsars below 100 MHz using LWA1. Astrophys J 2019;875:146. http://dx.doi.org/10.3847/1538-4357/ab0d8f, arXiv:1903.03457.

[123] Wu Z, Coles WA, Verbiest JPW, Ambalappat KM, Tiburzi C, Grießmeier JM, et al. Pulsar scintillation studies with LOFAR: II. Dual-frequency scattering study of PSR J0826+2637 with LOFAR and NenuFAR. Mon Not R Astron Soc 2023;520:5536–43. http://dx.doi.org/10.1093/mnras/stad429, arXiv:2302.02722.

[124] Geyer M, Karastergiou A, Kondratiev VI, Zagkouris K, Kramer M, Stappers BW, et al. Scattering analysis of LOFAR pulsar observations. Mon Not R Astron Soc 2017;470:2659–79. http://dx.doi.org/10.1093/mnras/stx1151, arXiv:1706.04205.

[125] Demorest PB. Cyclic spectral analysis of radio pulsars. Mon Not R Astron Soc 2011;416:2821–6. http://dx.doi.org/10.1111/j.1365-2966.2011.19230.x, arXiv:1106.3345.

[126] Dolch T, Stinebring DR, Jones G, Zhu H, Lynch RS, Cohen T, et al. Deconvolving pulsar signals with cyclic spectroscopy: A systematic evaluation. Astrophys J 2021;913:98. http://dx.doi.org/10.3847/1538-4357/abf48b, arXiv:2008.10562.

[127] Stinebring DR, McLaughlin MA, Cordes JM, Becker KM, Goodman JEE, Kramer MA, et al. Faint scattering around pulsars: Probing the interstellar medium on solar system size scales. Astrophys J 2001;549:L97–100.

[128] Ocker SK, Cordes JM, Chatterjee S, Stinebring DR, Dolch T, Pelgrims V, et al. Pulsar scintillation through thick and thin: Bow shocks, bubbles, and the broader interstellar medium. 2023, http://dx.doi.org/10.48550/arXiv.2309.13809, arXiv e-prints, arXiv:2309.13809.

[129] Hemberger DA, Stinebring DR. Time variability of interstellar scattering and improvements to pulsar timing. Astrophys J 2008;674:L37–40.

[130] Wu Z, Verbiest JPW, Main RA, Grießmeier JM, Liu Y, Osłowski S, et al. Pulsar scintillation studies with LOFAR. I. The census. Astron Astrophys 2022;663:A116. http://dx.doi.org/10.1051/0004-6361/202142980, arXiv:2203.10409.

[131] Main RA, Parthasarathy A, Johnston S, Karastergiou A, Basu A, Cameron AD, et al. The thousand pulsar array programme on MeerKAT - X. Scintillation arcs of 107 pulsars. Mon Not R Astron Soc 2023;518:1086–97. http://dx.doi.org/10.1093/mnras/stac3149, arXiv:2211.08471.

[132] Rosado PA, Sesana A, Gair J. Expected properties of the first gravitational wave signal detected with pulsar timing arrays. Mon Not R Astron Soc 2015;451:2417–33. http://dx.doi.org/10.1093/mnras/stv1098, arXiv:1503.04803.

[133] Kelley LZ, Blecha L, Hernquist L, Sesana A, Taylor SR. Single sources in the low-frequency gravitational wave sky: Properties and time to detection by pulsar timing arrays. Mon Not R Astron Soc 2018;477:964–76. http://dx.doi.org/10.1093/mnras/sty689, arXiv:1711.00075.

[134] Abbott BP, et al., KAGRA, LIGO Scientific, Virgo, VIRGO. Prospects for observing and localizing gravitational-wave transients with advanced LIGO, advanced Virgo and KAGRA. Living Rev. Rel. 2018;21:3. http://dx.doi.org/10.1007/s41114-020-00026-9, arXiv:1304.0670.

[135] Romano JD, Hazboun JS, Siemens X, Archibald AM. Common-spectrum process versus cross-correlation for gravitational-wave searches using pulsar timing arrays. Phys Rev D 2021;103:063027. http://dx.doi.org/10.1103/PhysRevD.103.063027, arXiv:2012.03804.

[136] Tiburzi C, Hobbs G, Kerr M, Coles WA, Dai S, Manchester RN, et al. A study of spatial correlations in pulsar timing array data. Mon Not R Astron Soc 2016;455:4339–50. http://dx.doi.org/10.1093/mnras/stv2143, arXiv:1510.02363.

[137] Goncharov B, Thrane E, Shannon RM, Harms J, Bhat NDR, Hobbs G, et al. Consistency of the parkes pulsar timing array signal with a nanohertz gravitational-wave background. Astrophys J 2022;932:L22. http://dx.doi.org/10.3847/2041-8213/ac76bb, arXiv:2206.03766.

[138] Allen B, Dhurandhar S, Gupta Y, McLaughlin M, Natarajan P, Shannon RM, Thrane E, Vecchio A. The international pulsar timing array checklist for the detection of nanohertz gravitational waves. 2023, http://dx.doi.org/10.48550/arXiv.2304.04767, arXiv e-prints, arXiv:2304.04767.

[139] Jenet FA, Hobbs GB, van Straten W, Manchester RN, Bailes M, Verbiest JPW, et al. Upper bounds on the low-frequency stochastic gravitational wave background from pulsar timing observations: Current limits and future prospects. Astrophys J 2006;653:1571–6. http://dx.doi.org/10.1086/508702, arXiv:astro-ph/0609013.

[140] Jaffe AH, Backer DC. Gravitational waves probe the coalescence rate of massive black hole binaries. Astrophys J 2003;583:616–31.

[141] Sesana A, Haardt F, Madau P, Volonteri M. Low-frequency gravitational radiation from coalescing massive black hole binaries in hierarchical cosmologies. Astrophys J 2004;611:623–32. http://dx.doi.org/10.1086/422185, arXiv:astro-ph/0401543.

[142] Shannon RM, Ravi V, Lentati LT, Lasky PD, Hobbs G, Kerr M, et al. Gravitational waves from binary supermassive black holes missing in pulsar observations. Science 2015;349:1522–5. http://dx.doi.org/10.1126/science.aab1910, arXiv:1509.07320.

[143] Reardon DJ, Zic A, Shannon RM, Hobbs GB, Bailes M, Di Marco V, et al. Search for an isotropic gravitational-wave background with the Parkes pulsar timing array. Astrophys J 2023;951:L6. http://dx.doi.org/10.3847/2041-8213/acdd02, arXiv:2306.16215.

[144] Arzoumanian Z, Baker PT, Brazier A, Burke-Spolaor S, Chamberlin SJ, Chatterjee S, et al., NANOGrav Collaboration. The NANOGrav 11 year data set: Pulsar-timing constraints on the stochastic gravitational-wave background. Astrophys J 2018;859:47. http://dx.doi.org/10.3847/1538-4357/aabd3b, arXiv:1801.02617.

[145] Lentati L, Taylor SR, Mingarelli CMF, Sesana A, Sanidas SA, Vecchio A, et al. European pulsar timing array limits on an isotropic stochastic gravitational-wave background. Mon Not R Astron Soc 2015;453:2576–98. http://dx.doi.org/10.1093/mnras/stv1538, arXiv:1504.03692.

[146] Champion DJ, Hobbs GB, Manchester RN, Edwards RT, Backer DC, Bailes M, et al. Measuring the mass of solar system planets using pulsar timing. Astrophys J 2010;720:L201–5. http://dx.doi.org/10.1088/2041-8205/720/2/L201, arXiv:1008.3607.

[147] Guo YJ, Lee KJ, Caballero RN. A dynamical approach in exploring the unknown mass in the solar system using pulsar timing arrays. Mon Not R Astron Soc 2018;475:3644–53. http://dx.doi.org/10.1093/mnras/stx3326, arXiv:1802.05452.

[148] Tinto M. Gravitational wave searches with pulsar timing arrays: Cancellation of clock and ephemeris noises. Phys Rev D 2018;97:084047. http://dx.doi.org/10.1103/PhysRevD.97.084047, arXiv:1802.09628.

[149] Roebber E. Ephemeris errors and the gravitational-wave signal: Harmonic mode coupling in pulsar timing array searches. Astrophys J 2019;876:55. http://dx.doi.org/10.3847/1538-4357/ab100e, arXiv:1901.05468.

[150] Park RS, Folkner WM, Williams JG, Boggs DH. The JPL planetary and lunar ephemerides DE440 and DE441. Astron J 2021;161:105. http://dx.doi.org/10.3847/1538-3881/abd414.

[151] Hazboun JS, Simon J, Siemens X, Romano JD. Model dependence of Bayesian gravitational-wave background statistics for pulsar timing arrays. Astrophys J 2020;905:L6. http://dx.doi.org/10.3847/2041-8213/abca92, arXiv:2009.05143.

[152] Johnson AD, Vigeland SJ, Siemens X, Taylor SR. Gravitational-wave statistics for pulsar timing arrays: Examining bias from using a finite number of pulsars. Astrophys J 2022;932:105. http://dx.doi.org/10.3847/1538-4357/ac6f5e, arXiv:2201.10657.

[153] van Haasteren R, Levin Y, Janssen GH, Lazaridis K, Kramer M, Stappers BW, et al. Placing limits on the stochastic gravitational-wave background using European pulsar timing array data. Mon Not R Astron Soc 2011;414:3117–28. http://dx.doi.org/10.1111/j.1365-2966.2011.18613.x, arXiv:1103.0576.

[154] Shannon RM, Ravi V, Coles WA, Hobbs G, Keith MJ, Manchester RN, et al. Gravitational-wave limits from pulsar timing constrain supermassive black hole evolution. Science 2013;342:334–7, arXiv:1310.4569.

[155] Arzoumanian Z, Brazier A, Burke-Spolaor S, Chamberlin SJ, Chatterjee S, Christy B, et al., NANOGrav Collaboration. The NANOGrav nine-year data set: Limits on the isotropic stochastic gravitational wave background. Astrophys J 2016;821:13. http://dx.doi.org/10.3847/0004-637X/821/1/13, arXiv:1508.03024.

[156] Goncharov B, Shannon RM, Reardon DJ, Hobbs G, Zic A, Bailes M, et al. On the evidence for a common-spectrum process in the search for the nanohertz gravitational-wave background with the parkes pulsar timing array. Astrophys J 2021;917:L19. http://dx.doi.org/10.3847/2041-8213/ac17f4, arXiv:2107.12112.

[157] Chen S, Caballero RN, Guo YJ, Chalumeau A, Liu K, Shaifullah G, et al. Common-red-signal analysis with 24-yr high-precision timing of the European pulsar timing array: Inferences in the stochastic gravitational-wave background search. Mon Not R Astron Soc 2021;508:4970–93. http://dx.doi.org/10.1093/mnras/stab2833, arXiv:2110.13184.

[158] Antoniadis J, Arzoumanian Z, Babak S, Bailes M, Bak Nielsen AS, Baker PT, et al. The international pulsar timing array second data release: Search for an isotropic gravitational wave background. Mon Not R Astron Soc 2022;510:4873–87. http://dx.doi.org/10.1093/mnras/stab3418, arXiv:2201.03980.
[159] Agazie G, Anumarlapudi A, Archibald AM, Arzoumanian Z, Baker PT, Bécsy B, et al., Nanograv Collaboration. The NANOGrav 15 yr data set: Evidence for a gravitational-wave background. Astrophys J 2023;951:L8. http://dx.doi.org/10.3847/2041-8213/acdac6, arXiv:2306.16213.
[160] EPTA Collaboration and InPTA Collaboration Antoniadis J, Arumugam P, Arumugam S, Babak S, Bagchi M, Bak Nielsen AS, et al. The second data release from the European pulsar timing array. III. Search for gravitational wave signals. Astron Astrophys 2023;678:A50. http://dx.doi.org/10.1051/0004-6361/202346844, arXiv:2306.16214.
[161] Zic A, Hobbs G, Shannon RM, Reardon D, Goncharov B, Bhat NDR, et al. Evaluating the prevalence of spurious correlations in pulsar timing array data sets. Mon Not R Astron Soc 2022;516:410–20. http://dx.doi.org/10.1093/mnras/stac2100, arXiv:2207.12237.
[162] Chalumeau A, Babak S, Petiteau A, Chen S, Samajdar A, Caballero RN, et al. Noise analysis in the European pulsar timing array data release 2 and its implications on the gravitational-wave background search. Mon Not R Astron Soc 2022;509:5538–58. http://dx.doi.org/10.1093/mnras/stab3283, arXiv:2111.05186.
[163] Bernardo RC, Ng KW. Pulsar and cosmic variances of pulsar timing-array correlation measurements of the stochastic gravitational wave background. J Cosmol Astropart Phys 2022;2022:046. http://dx.doi.org/10.1088/1475-7516/2022/11/046, arXiv:2209.14834.
[164] Allen B. Variance of the Hellings-Downs correlation. Phys Rev D 2023;107:043018. http://dx.doi.org/10.1103/PhysRevD.107.043018, arXiv:2205.05637.
[165] Allen B, Romano JD. Hellings and downs correlation of an arbitrary set of pulsars. Phys Rev D 2023;108:043026. http://dx.doi.org/10.1103/PhysRevD.108.043026, arXiv:2208.07230.
[166] Romano JD, Allen B. Answers to frequently asked questions about the pulsar timing array hellings and downs correlation curve. 2023, http://dx.doi.org/10.48550/arXiv.2308.05847, arXiv e-prints, arXiv:2308.05847.
[167] Perera BBP, Stappers BW, Babak S, Keith MJ, Antoniadis J, Bassa CG, et al. Improving timing sensitivity in the microhertz frequency regime: Limits from PSR J1713+0747 on gravitational waves produced by supermassive black hole binaries. Mon Not R Astron Soc 2018;478:218–27. http://dx.doi.org/10.1093/mnras/sty1116, arXiv:1804.10571.
[168] Falxa M, Babak S, Baker PT, Bécsy B, Chalumeau A, Chen S, et al., IPTA Collaboration. Searching for continuous gravitational waves in the second data release of the international pulsar timing array. Mon Not R Astron Soc 2023;521:5077–86. http://dx.doi.org/10.1093/mnras/stad812, arXiv:2303.10767.
[169] Antoniadis J, Arumugam P, Arumugam S, Babak S, Bagchi M, Bak Nielsen AS, Bassa CG, et al. The second data release from the European pulsar timing array IV. Search for continuous gravitational wave signals. 2023, http://dx.doi.org/10.48550/arXiv.2306.16226, arXiv e-prints, arXiv:2306.16226.
[170] Agazie G, Anumarlapudi A, Archibald AM, Arzoumanian Z, Baker PT, Bécsy B, et al., Nanograv Collaboration. The NANOGrav 15 yr data set: Bayesian limits on gravitational waves from individual supermassive black hole binaries. Astrophys J 2023;951:L50. http://dx.doi.org/10.3847/2041-8213/ace18a, arXiv:2306.16222.
[171] Taylor SR, Huerta EA, Gair JR, McWilliams ST. Detecting eccentric supermassive black hole binaries with pulsar timing arrays: Resolvable source strategies. Astrophys J 2016;817:70. http://dx.doi.org/10.3847/0004-637X/817/1/70, arXiv:1505.06208.
[172] Susobhanan A, Gopakumar A, Hobbs G, Taylor SR. Pulsar timing array signals induced by black hole binaries in relativistic eccentric orbits. Phys Rev D 2020;101:043022. http://dx.doi.org/10.1103/PhysRevD.101.043022, arXiv:2002.03285.
[173] Susobhanan A. Post-Newtonian-accurate pulsar timing array signals induced by inspiralling eccentric binaries: Accuracy, computational cost, and single-pulsar search. Classical Quantum Gravity 2023;40:155014. http://dx.doi.org/10.1088/1361-6382/ace234, arXiv:2210.11454.
[174] Agazie G, Arzoumanian Z, Baker PT, Bécsy B, Blecha L, Blumer H, Brazier A, et al. The NANOGrav 12.5-year data set: Multi-messenger targeted search for gravitational waves from an eccentric supermassive binary in 3C 66b. 2023, http://dx.doi.org/10.48550/arXiv.2309.17438, arXiv e-prints, arXiv:2309.17438.
[175] Sudou H, Iguchi S, Murata Y, Taniguchi Y. Orbital motion in the radio galaxy 3C 66b: Evidence for a supermassive black hole binary. Science 2003;300:1263–5. http://dx.doi.org/10.1126/science.1082817.
[176] Sesana A. Gravitational wave emission from binary supermassive black holes. Classical Quantum Gravity 2013;30:244009. http://dx.doi.org/10.1088/0264-9381/30/24/244009, arXiv:1307.4086.
[177] Gardiner EC, Kelley LZ, Lemke AM, Mitridate A. Beyond the background: Gravitational wave anisotropy and continuous waves from supermassive black hole binaries. 2023, http://dx.doi.org/10.48550/arXiv.2309.07227, arXiv e-prints, arXiv:2309.07227.
[178] Pol N, Taylor SR, Romano JD. Forecasting pulsar timing array sensitivity to anisotropy in the stochastic gravitational wave background. Astrophys J 2022;940:173. http://dx.doi.org/10.3847/1538-4357/ac9836, arXiv:2206.09936.
[179] Siemens X, Ellis J, Jenet F, Romano JD. The stochastic background: Scaling laws and time to detection for pulsar timing arrays. Classical Quantum Gravity 2013;30:224015. http://dx.doi.org/10.1088/0264-9381/30/22/224015, arXiv:1305.3196.
[180] Agazie G, Anumarlapudi A, Archibald AM, Arzoumanian Z, Baker PT, Bécsy B, et al. The NANOGrav 15 yr data set: Search for anisotropy in the gravitational-wave background. Astrophys J 2023;956:L3. http://dx.doi.org/10.3847/2041-8213/acf4fd, arXiv:2306.16221.
[181] D'Orazio DJ, Charisi M. Observational signatures of supermassive black hole binaries. 2023, http://dx.doi.org/10.48550/arXiv.2310.16896, arXiv e-prints, arXiv:2310.16896.
[182] Agazie G, Anumarlapudi A, Archibald AM, Baker PT, Bécsy B, Blecha L, et al., Nanograv Collaboration. The NANOGrav 15 yr data set: Constraints on supermassive black hole binaries from the gravitational-wave background. Astrophys J 2023;952:L37. http://dx.doi.org/10.3847/2041-8213/ace18b, arXiv:2306.16220.
[183] Antoniadis J, Arumugam P, Arumugam S, Auclair P, Babak S, Bagchi M, et al. The second data release from the European pulsar timing array: V. Implications for massive black holes, dark matter and the early universe. 2023, http://dx.doi.org/10.48550/arXiv.2306.16227, arXiv e-prints, arXiv:2306.16227.
[184] Henriques BMB, White SDM, Thomas PA, Angulo R, Guo Q, Lemson G, et al. Galaxy formation in the Planck cosmology - I. Matching the observed evolution of star formation rates, colours and stellar masses. Mon Not R Astron Soc 2015;451:2663–80. http://dx.doi.org/10.1093/mnras/stv705, arXiv:1410.0365.
[185] Izquierdo-Villalba D, Sesana A, Bonoli S, Colpi M. Massive black hole evolution models confronting the n-hz amplitude of the stochastic gravitational wave background. Mon Not R Astron Soc 2022;509:3488–503. http://dx.doi.org/10.1093/mnras/stab3239, arXiv:2108.11671.
[186] Valtolina S, Shaifullah G, Samajdar A, Sesana A. Testing strengths, limitations and biases of current pulsar timing arrays detection analyses on realistic data. 2023, http://dx.doi.org/10.48550/arXiv.2309.13117, arXiv e-prints, arXiv:2309.13117.
[187] Bécsy B, Cornish NJ, Meyers PM, Kelley LZ, Agazie G, Anumarlapudi A, et al. How to detect an astrophysical nanohertz gravitational-wave background. 2023, http://dx.doi.org/10.48550/arXiv.2309.04443, arXiv e-prints, arXiv:2309.04443.
[188] Lino dos Santos RR, van Manen LM. Gravitational waves from the early universe. 2022, http://dx.doi.org/10.48550/arXiv.2212.05594, arXiv e-prints, arXiv:2212.05594.
[189] Afzal A, Agazie G, Anumarlapudi A, Archibald AM, Arzoumanian Z, Baker PT, et al., Nanograv Collaboration. The NANOGrav 15 yr data set: Search for signals from new physics. Astrophys J 2023;951:L11. http://dx.doi.org/10.3847/2041-8213/acdc91, arXiv:2306.16219.
[190] Vagnozzi S. Inflationary interpretation of the stochastic gravitational wave background signal detected by pulsar timing array experiments. J High Energy Astrophys 2023;39:81–98. http://dx.doi.org/10.1016/j.jheap.2023.07.001, arXiv:2306.16912.
[191] Khoury J, Ovrut BA, Steinhardt PJ, Turok N. Ekpyrotic universe: Colliding branes and the origin of the hot big bang. Phys Rev D 2001;64:123522. http://dx.doi.org/10.1103/PhysRevD.64.123522, arXiv:hep-th/0103239.
[192] Khmelnitsky A, Rubakov V. Pulsar timing signal from ultralight scalar dark matter. J Cosmol Astropart Phys 2014;2:19. http://dx.doi.org/10.1088/1475-7516/2014/02/019, arXiv:1309.5888.
[193] Porayko NK, Zhu X, Levin Y, Hui L, Hobbs G, Grudskaya A, et al., PPTA Collaboration. Parkes pulsar timing array constraints on ultralight scalar-field dark matter. Phys Rev D 2018;98:102002. http://dx.doi.org/10.1103/PhysRevD.98.102002, arXiv:1810.03227.
[194] Smarra C, Goncharov B, Barausse E, Antoniadis J, Babak S, Nielsen ASB, et al., European Pulsar Timing Array. Second data release from the European pulsar timing array: Challenging the ultralight dark matter paradigm. Phys Rev Lett 2023;131:171001. http://dx.doi.org/10.1103/PhysRevLett.131.171001, arXiv:2306.16228.
[195] Kaplan DE, Mitridate A, Trickle T. Constraining fundamental constant variations from ultralight dark matter with pulsar timing arrays. Phys Rev D 2022;106:035032. http://dx.doi.org/10.1103/PhysRevD.106.035032, arXiv:2205.06817.
[196] Graham PW, Mardon J, Rajendran S. Vector dark matter from inflationary fluctuations. Phys Rev D 2016;93:103520. http://dx.doi.org/10.1103/PhysRevD.93.103520, arXiv:1504.02102.
[197] Xue X, Xia ZQ, Zhu X, Zhao Y, Shu J, Yuan Q, et al., PPTA Collaboration. High-precision search for dark photon dark matter with the parkes pulsar timing array. Phys Rev Res 2022;4:L012022. http://dx.doi.org/10.1103/PhysRevResearch.4.L012022, arXiv:2112.07687.
[198] Hees A, Guéna J, Abgrall M, Bize S, Wolf P. Searching for an oscillating massive scalar field as a dark matter candidate using atomic hyperfine frequency comparisons. Phys Rev Lett 2016;117:061301. http://dx.doi.org/10.1103/PhysRevLett.117.061301, arXiv:1604.08514.

[199] Optical Network, B.A.C., Collaboration Beloy K, Bodine MI, Bothwell T, Brewer SM, Bromley SL, Chen JS, et al. Frequency ratio measurements with 18-digit accuracy using a network of optical clocks. 2020, http://dx.doi.org/10.48550/arXiv.2005.14694, arXiv e-prints, arXiv:2005.14694, arXiv:2005.14694.

[200] Bergé J, Brax P, Métris G, Pernot-Borràs M, Touboul P, Uzan JP. MICROSCOPE mission: First constraints on the violation of the weak equivalence principle by a light scalar dilaton. Phys Rev Lett 2018;120:141101. http://dx.doi.org/10.1103/PhysRevLett.120.141101, arXiv:1712.00483.

[201] Chatziioannou K, Yunes N, Cornish N. Model-independent test of general relativity: An extended post-Einsteinian framework with complete polarization content. Phys Rev D 2012;86:022004. http://dx.doi.org/10.1103/PhysRevD.86.022004, arXiv:1204.2585.

[202] Pang PTH, Lo RKL, Wong ICF, Li TGF, Van Den Broeck C. Generic searches for alternative gravitational wave polarizations with networks of interferometric detectors. Phys Rev D 2020;101:104055. http://dx.doi.org/10.1103/PhysRevD.101.104055, arXiv:2003.07375.

[203] Abbott R, Abbott TD, Abraham S, Acernese F, Ackley K, Adams A, et al. Tests of general relativity with binary black holes from the second LIGO-Virgo gravitational-wave transient catalog. Phys Rev D 2021;103:122002. http://dx.doi.org/10.1103/PhysRevD.103.122002, arXiv:2010.14529.

[204] The LIGO Scientific Collaboration and the Virgo Collaboration and the KAGRA Collaboration Abbott R, Abe H, Acernese F, Ackley K, Adhikari N, Adhikari RX, et al. Tests of general relativity with GWTC-3. 2021, http://dx.doi.org/10.48550/arXiv.2112.06861, arXiv e-prints, arXiv:2112.06861.

[205] Magaña Hernandez I. Measuring the polarization content of gravitational waves with strongly lensed binary black hole mergers. 2022, http://dx.doi.org/10.48550/arXiv.2211.01272, arXiv e-prints, arXiv:2211.01272.

[206] Chatziioannou K, Isi M, Haster CJ, Littenberg TB. Morphology-independent test of the mixed polarization content of transient gravitational wave signals. Phys Rev D 2021;104:044005. http://dx.doi.org/10.1103/PhysRevD.104.044005, arXiv:2105.01521.

[207] Lee KJ, Jenet FA, Price RH. Pulsar timing as a probe of non-Einsteinian polarizations of gravitational waves. Astrophys J 2008;685:1304–19.

[208] Cornish NJ, O'Beirne L, Taylor SR, Yunes N. Constraining alternative theories of gravity using pulsar timing arrays. Phys Rev Lett 2018;120:181101. http://dx.doi.org/10.1103/PhysRevLett.120.181101, arXiv:1712.07132.

[209] Wu YM, Chen ZC, Huang QG. Constraining the polarization of gravitational waves with the parkes pulsar timing array second data release. Astrophys J 2022;925:37. http://dx.doi.org/10.3847/1538-4357/ac35cc, arXiv:2108.10518.

[210] Agazie G, Anumarlapudi A, Archibald AM, Arzoumanian Z, Baier J, Baker PT, et al. The NANOGrav 15-year data set: Search for transverse polarization modes in the gravitational-wave background. 2023, http://dx.doi.org/10.48550/arXiv.2310.12138, arXiv e-prints, arXiv:2310.12138.

[211] Moore CJ, Taylor SR, Gair JR. Estimating the sensitivity of pulsar timing arrays. Classical Quantum Gravity 2015;32:055004. http://dx.doi.org/10.1088/0264-9381/32/5/055004, arXiv:1406.5199.

[212] Good D, International Pulsar Timing Array Team. Creating a new international pulsar timing array dataset. In: American astronomical society meeting abstracts. 2023, p. 438.02.

[213] Graikou E, Verbiest JPW, Osłowski S, Champion DJ, Tauris TM, Jankowski F, Kramer M. Limits on the mass, velocity and orbit of PSR J1933-6211. Mon Not R Astron Soc 2017;471:4579–86. http://dx.doi.org/10.1093/mnras/stx1795, arXiv:1708.01819.

[214] Geyer M, Venkatraman Krishnan V, Freire PCC, Kramer M, Antoniadis J, Bailes M, et al. Mass measurements and 3D orbital geometry of PSR J1933-6211. Astron Astrophys 2023;674:A169. http://dx.doi.org/10.1051/0004-6361/202244654, arXiv:2304.09060.

[215] Hu H, Kramer M, Champion DJ, Wex N, Parthasarathy A, Pennucci TT, et al. Gravitational signal propagation in the double pulsar studied with the MeerKAT telescope. Astron Astrophys 2022;667:A149. http://dx.doi.org/10.1051/0004-6361/202244825, arXiv:2209.11798.

[216] Bailes M, Jameson A, Abbate F, Barr ED, Bhat NDR, Bondonneau L, et al. The MeerKAT telescope as a pulsar facility: System verification and early science results from MeerTime. PASA 2020;37:e028. http://dx.doi.org/10.1017/pasa.2020.19, arXiv:2005.14366.

[217] Nan R, Li D, Jin C, Wang Q, Zhu L, Zhu W, et al. The five-hundred aperture spherical radio telescope (fast) project. Internat J Modern Phys D 2011;20:989–1024. http://dx.doi.org/10.1142/S0218271811019335, arXiv:1105.3794.

[218] Hallinan G, Ravi V, Weinreb S, Kocz J, Huang Y, Woody DP, et al. The DSA-2000 —A radio survey camera. Bull Am Astron Soc 2019;255. http://dx.doi.org/10.48550/arXiv.1907.07648, arXiv:1907.07648.

[219] Manchester RN, Hobbs GB, Teoh A, Hobbs M. The Australia telescope national facility pulsar catalogue. Astron J 2005;129:1993–2006.

[220] Laal N, Lamb WG, Romano JD, Siemens X, Taylor SR, van Haasteren R. Exploring the capabilities of Gibbs sampling in pulsar timing arrays. Phys Rev D 2023;108:063008. http://dx.doi.org/10.1103/PhysRevD.108.063008, arXiv:2305.12285.

[221] Shih D, Freytsis M, Taylor SR, Dror JA, Smyth N. Fast parameter inference on pulsar timing arrays with normalizing flows. 2023, http://dx.doi.org/10.48550/arXiv.2310.12209, arXiv e-prints, arXiv:2310.12209.

[222] Fiore W, Levin L, McLaughlin MA, Anumarlapudi A, Kaplan DL, Swiggum JK, et al. The green bank north celestial cap survey. VIII. 21 new pulsar timing solutions. Astrophys J 2023;956:40. http://dx.doi.org/10.3847/1538-4357/aceef7, arXiv:2305.13624.